Comparative Transcriptomic Analysis of Perfluoroalkyl Substances-Induced Responses of Exponential and Stationary Phase *Escherichia coli*

Molly E. Wintenberg,[a]# Olga B. Vasilyeva,[a] Samuel W. Schaffter[a]

[a] Material Measurement Laboratory, National Institute of Standards and Technology, U.S. Department of Commerce, Gaithersburg, Maryland, USA

Running head: Temporal Transcriptomic Responses of *E. coli* to PFCAs

(53 characters with spaces)

#Address correspondence to Molly E. Wintenberg, molly.wintenberg@nist.gov

Abstract word count: 250

ABSTRACT

Per- and polyfluoroalkyl substances (PFAS) are highly stable chemical contaminants of emerging concern for human and environmental health due to their non-natural chemistry, widespread use, and environmental persistence. Despite conventional metrology, mitigation strategies, and removal technologies, the complexity of this growing problem necessitates the need for alternative approaches to tackle the immense challenges associated with complex environmental PFAS contamination. Recently, biology has emerged as an alternative approach to detect and mitigate PFAS and understand the molecular-level responses of living organisms, including microorganisms, to these compounds. However, further study is needed to understand how microorganisms in different environments and growth phases respond to PFAS. In this study, we performed RNA sequencing at mid-exponential, early stationary phase, and late stationary phase of bacterial growth to determine the global transcriptional response of a model chassis, *Escherichia coli* MG1655, induced by two PFAS, perfluorooctanoic acid (PFOA) and perfluorododecanoic acid (PFDoA), and equivalent non-fluorinated carboxylic acids (NFCA), octanoic acid and dodecanoic acid. Differential gene expression analysis revealed PFOA and PFDoA induced distinct changes in gene expression throughout cultivation. Specifically, we identified significant changes in expression of the formate regulon and sulfate assimilation at mid-exponential phase and ferrous iron transport, central metabolism, the molecular chaperone network, and motility processes during stationary phase. Importantly, many of these changes are not induced by NFCAs. In summary, we found PFAS induced a system-level change in gene expression, and our results expand the understanding of bacterial-PFAS interactions that could enable the development of future real-time environmental monitoring and mitigation technologies.

38 **Importance**

39 The prevalence and persistence of PFAS in the environment is a growing area of concern.
40 However, little is understood of the impacts of PFAS on the environment, particularly impacts on
41 microorganisms that play pivotal roles in nearly every ecosystem. Thus, comprehensive
42 measurements that provide systems-level insight into how microorganisms respond and adapt to
43 PFAS in the environment are paramount. Here, we use RNA sequencing to study the global
44 transcriptional response of *E. coli* MG1655 to two PFAS and non-fluorinated equivalent
45 compounds across growth phases. We find that PFAS induce system-level changes in metabolic,
46 transport, and gene regulatory pathways, providing insight into how these non-natural chemicals
47 interact with a model bacterium. Additionally, the transcriptomic dataset associated with this work
48 provides the community with PFSA-specific gene expression patterns and possible PFAS
49 degradation pathways for the development of future whole-cell biosensors and mitigation efforts.

50 **INTRODUCTION**

51 Per- and polyfluoroalkyl substances (PFAS) are a class of fluorinated compounds with various
52 structures conferring strong resistance to degradation or decomposition in the environment (1).
53 Widespread industrial production of fire-fighting foam and non-stick coatings and use in other
54 consumer products of pesticides, cleaning materials, and personal care products, has led to
55 substantial release of PFAS into the environment, raising concerns about their environmental
56 persistence and bioaccumulation (2, 3). PFAS have been detected ubiquitously in human hair,
57 breast milk, and blood and in environmental populations, such as water basins, surface soils, and
58 plants cultivated in contaminated sites (4-10). Exposure to PFAS has been linked to several adverse
59 human health effects, including immunotoxicity, liver damage, and thyroid disfunction and
60 negative ecological impacts of endocrine disruption in aquatic species (11-14).

To date, the U. S. Environmental Protection Agency (USEPA) and the international Organization of Economic Co-operation and Development (OECD) have categorized thousands of individual compounds based on a threshold of fluorine percentage and molecular structure or the presence of perfluoroalkyl moieties (15, 16). The structures of these compounds are distinct with linear and branched carbon chains of varying length and fluorination and functional head groups containing sulfonates, sulfonamides, carboxylates, and other moieties that are believed to govern compound stability, transport, and environmental fate (17). In addition to the variety of PFAS across industrial products, environmental samples from a single contaminated source will often contain mixtures of intact PFAS, partial degradation products, and precursor chemicals (18, 19). Sample complexity and batch variation make measurement and quantitation of PFAS-containing samples with traditional analytical techniques like liquid chromatography – mass spectrometry (LC-MS) (20-22) challenging and costly. Moreover, water remediation strategies including ion exchange resins, high-pressure membrane systems, and granular activated carbon (23) and soil remediation strategies including thermal treatment and soil washing (24) are also complicated by the unique chemical properties that originally made PFAS efficient in industrial and commercial products. To rapidly respond to this growing problem, there is a need for alternative approaches to real-time environmental monitoring and mitigation efforts, as well as comprehensive methods to assess environmental impact (25-27). Increasingly, researchers are turning to biology as an alternative approach for PFAS detection (28, 29) and mitigation (25, 30). Broad measurements of living systems could not only aid in rapid, on-site detection of new contamination sources and identification and classification of new PFAS byproducts but also expand our general understanding of the biological consequences of PFAS contamination (25, 26).

Bacteria are a promising measurement platform as they play critical roles in most

84 ecosystems, are highly concentrated in soil environments and aquifers where PFAS contamination
85 persists (31, 32), and rapidly sense and respond to environmental fluctuations (33, 34).
86 Transcriptomic analysis by RNA sequencing (RNA-seq) of bacterial interactions with PFAS could
87 serve as an alternative measurement strategy to explore genome-wide molecular mechanisms
88 underlying gene expression level changes induced by PFAS. RNA-seq is a widely applicable
89 technique that can investigate the response of a wide variety of organisms to various types and
90 mixtures of PFAS, potentially enabling the identification of specific sensing gene targets and PFAS
91 degradation pathways and provide insight into how these non-natural chemicals interact with
92 living systems. Although, omics-based analyses have been used to examine the biological response
93 of several organisms, including primary human liver cell spheroids, zebrafish, and *Escherichia*
94 *coli*, to various PFAS (35-38), studies exploring the global transcriptional response of bacteria
95 across key growth phases are limited.

96 In this study, we employed time course RNA-seq at key phases of bacterial growth to
97 investigate the global transcriptional response of a model Gram-negative bacterium, *E. coli*
98 MG1655, to PFAS (Figure 1). *E. coli* is an optimal organism to begin understanding the microbial
99 transcriptional responses to PFAS, as it is present in different environments and its transcriptional
100 responses to numerous stressors and growth conditions have been extensively studied with RNA-
101 seq (39-42). *E. coli* was grown in the presence of perfluoroalkyl carboxylic acids (PFCA) or
102 equivalent non-fluorinated carboxylic acids (NFCA) at a concentration of 100 μmol/L for 48 hr,
103 and samples were sequenced at mid-exponential and stationary phase. Differential expression
104 analysis revealed significant changes in mid-exponential and stationary phase gene expression
105 induced by two different PFCAs, including changes that differed from the NFCAs. Our results
106 indicate *E. coli* employed different mechanisms at different growth phases further signifying

107 temporal gene expression in response to PFCAs. Specifically, we identified significant changes in
108 the expression of the formate regulon and sulfate assimilation at mid-exponential phase, ferrous
109 iron transport, amino acid metabolism, small regulatory RNAs during early stationary phase, and
110 central metabolism, ribosome biosynthesis, molecular chaperones, sigma factors, and motility
111 process of flagellar assembly and chemotaxis during late stationary phase. The transcription-level
112 responses of *E. coli* to PFCAs presented in this study expand our knowledge of the molecular-level
113 response to PFAS and could inform the development of future environmental monitoring and
114 mitigation strategies.

115 **RESULTS AND DISCUSSION**

116 **Culturing *E. coli* with 100 μmol/L of PFCA does not inhibit growth**

117 To study the transcriptional responses of *E. coli* to PFAS, we first needed to understand the
118 growth characteristics of *E. coli* in the presence of PFAS. From a sub-class of PFAS, two PFCAs,
119 perfluorooctanoic acid (PFOA) and perfluorododecanoic acid (PFDoA), were selected as
120 representative PFCAs commonly found in environmental contamination (12, 43) and to provide a
121 comparison of chain length of PFCAs between 8 and 12 carbons, respectively (Figure 2 A). We
122 aimed to select a concentration high enough to induce a measurable change in gene expression but
123 low enough to avoid toxicity to the cells. Based on existing literature (37, 44) and the observation
124 that *E. coli* cell division and growth can stall with fluoride concentrations between 10 μmol/L and
125 100 μmol/L (45-47), we initially selected these concentrations to explore PFOA and PFDoA
126 toxicity. *E. coli* was grown in M9 minimal medium supplemented with glucose and 10 μmol/L or
127 100 μmol/L of either PFOA or PFDoA for a period of 48 hours at 37 °C (SI Figure 1, Materials
128 and Methods). The PFCAs were dissolved in dimethyl sulfoxide (DMSO), so to generate untreated
129 control samples for differential expression analysis, cells were cultivated in the same liquid

130 medium with an equal concentration of DMSO not containing PFCAs. NFCAs, octanoic acid (OA)
131 and dodecanoic acid (DoA) (Figure 2 A), were also included to compare the response of *E. coli* to
132 fluorinated and non-fluorinated carboxylic acids. All sample groups were prepared in biological
133 triplicate (SI Figure 1). We monitored growth of *E. coli* in the presence and absence of PFCAs or
134 NFCAs using optical density measurements at 600 nm (OD_{600}) at select time points (Figure 2 B;
135 SI Figure 2) across 48 hours. *E. coli* exhibited similar growth profiles for both 100 µmol/L (Figure
136 2 B) and 10 µmol/L (SI Figure 2) of PFOA, PFDoA, OA, and DoA, and a two-way mixed ANOVA
137 confirmed no statistically significant difference in growth to the untreated control (Table SI 1). As
138 both concentrations tested yielded similar growth profiles, we elected to collect samples for
139 sequencing and downstream analysis from cells grown with 100 µmol/L of each compound.

140 **Global transcriptional response of *E. coli* to PFCAs and NFCAs across the time course**

141 Next, we collected samples for total RNA extraction and next generation sequencing (NGS)
142 at 6 hr, 24 hr, and 48 hr. Sampling times were selected to represent mid-exponential phase, the
143 transition from exponential to stationary phase, and the end of stationary phase of bacterial growth.
144 Gene expression naturally shifts between these growth phases (48); therefore, we hypothesize
145 PFCAs will further exaggerate the natural changes in expression. We extracted total RNA from
146 three biologically distinct cultures of each sample type for commercial cDNA library preparation
147 and sequencing (Materials and Methods). NGS generated a total of over 350 million reads with a
148 mean quality score of 35.88 (Table SI 2).

149 We performed principal component analysis (PCA) of normalized data through DESeq2
150 methodology (49) to visualize variation in gene expression between the 45 samples in this study
151 (SI Figure 3). All transcriptomes first cluster with their respective growth phase as seen with PC1,
152 implying an inherent temporal transcriptomic response. Transcriptomes of 24 hr and 48 hr samples

153 had less variation and clustered closer to one another than to the 6 hr transcriptomes, suggesting
154 gene expression during the two points within stationary phase was more similar than mid-
155 exponential phase at the time of sampling. These results demonstrate the global shift in gene
156 expression is governed by a shift from active growth to cell survival and response to stress
157 regardless of sample type. Additionally, PFOA samples clustered more closely to PFDoA samples
158 than the untreated control samples throughout the time course (SI Figure 3), indicating additional
159 difference in gene expression was likely induced by PFCAs. At 6 hr and 24 hr, NFCA
160 transcriptomes clustered more closely to untreated control transcriptomes than PFCA
161 transcriptomes, suggesting gene expression of NFCAs and untreated samples were more similar
162 compared to PFCA samples. PCA indicated a biological replicate of DoA at 48 hr had a large
163 variation in gene expression from the triplicate group (outlier); as a result, DoA triplicate samples
164 at 48 hr were removed from further analysis.

165 We employed differential gene expression analysis to determine if PFCAs induced a
166 measurable change in *E. coli* gene expression over the time course. In this study, we consider genes
167 to be differentially expressed if the adjusted p-value (padj) is less than 0.05. Additionally, we mark
168 moderate and significant differential expression with absolute values of the $\log_2$ fold change
169 greater than or equal to 1.2 and 1.5, respectively. Untreated samples serve as the reference level
170 for gene expression pairwise comparisons. The global transcriptional response of *E. coli* to PFOA
171 and PFDoA demonstrates a measurable change in gene expression was induced by both PFCAs
172 throughout the time course (Figure 3 A, B). A similar number of genes were differentially
173 expressed by PFOA and PFDoA at 6 hr and 24 hr (Figure 4 A). However, this trend diverges at 48
174 hr, as PFOA induced the most differentially expressed genes and PFDoA induced the least. The
175 considerable change in gene expression induced at 48 hr by PFOA could be due to many factors,

176 which we will explore in more detail in later sections. NFCAs also induced a measurable change
177 in gene expression when compared to the untreated control across the time course (Figure 4 B; SI
178 Figure 4 A, B). *E. coli* grown with OA exhibited a similar pattern of expression to PFOA at 6 hr
179 and 24 hr (SI Figure 5 A). However, PFOA induced differential expression of more than 700 genes
180 at 48 hr, in contrast, OA induced less than 40 genes (SI Figure 5 B), indicating differed response
181 to fluorinated and non-fluorinated versions of the 8-chain compound. DoA had an opposite result
182 from PFDoA, inducing differential expression in over 350 genes compared to over 50 genes at 6
183 hr (Figure 4 A, B; SI Figure 5 C), further suggesting differed responses to fluorinated and non-
184 fluorinated versions of the 12-chain compound.

185 We observed a temporal pattern to PFCA- and NFCA-induced differential expression, as
186 the majority of genes were significantly changed at only one time point (Figure 4 C, D). Less than
187 30 and 15 genes were differentially expressed at multiple time points by PFOA and PFDoA,
188 respectively (Table SI 3; Table SI 4). Only three genes*, gatD, glpA*, and *yeaR,* which are related to
189 galactose metabolism and transport (50) and glycerol metabolism (51), were differentially
190 expressed by PFOA at all time points in the study (Figure 4 C top ; Table SI 3). Genes encoding
191 formate hydrogenlyase subunits, iron transporters, and small regulatory RNAs were differentially
192 expressed by PFOA at two of the three time points and will be discussed in later sections. Unlike
193 PFOA, no genes were differentially expressed in *E. coli* by PFDoA at all time points (Figure 4 C
194 bottom). Upon further investigation, nine genes, including the *trp* operon, downregulated by
195 PFDoA at 6 hr and 24 hr, were also downregulated by PFOA and OA at 24 hr and DoA at 6 hr (SI
196 Figure 5 D, E; Table SI 5), and will be discussed in a later section. Also discussed later, three of
197 the four genes upregulated by PFDoA at 6 hr and 24 hr were also downregulated by PFOA at 24
198 hr and 48 hr and OA at 6 hr (Table SI 5). These genes compose the ferrous iron transport operon,

199 *feo*ABC. Similar to PFOA, we observed a temporal pattern of OA-induced differential expression
200 over the time course with minimal common expression between time points (Figure 4 B, D top;
201 Table SI 6). Throughout the time course, PFOA and OA induced 13, 32, and 35 of the same genes
202 at 6 hr, 24 hr, and 48 hr, respectively (SI Figure 5 A, B; Table SI 7). These results suggest responses
203 were triggered by the octanoic acid moiety regardless of fluorination. Additionally, DoA
204 commonly induced differential expression in two genes, *prpC* and *ydeO*, involved in propionate
205 catabolism (52) and regulation of the *gad* system (53), at 6 hr and 24 hr (Figure 4 D bottom; Table
206 SI 8), similar to minimal shared expression of 9 genes by PFDoA at 6 hr and 24 hr (Figure 4 C
207 bottom; SI Figure 5 C; Table SI 4). Parallel to common expression between PFOA and OA, PFDoA
208 and DoA induced differential expression in the same 19 genes at 6 hr and 13 other genes at 24 hr
209 (SI Figure 5 C; Table SI 7). These results indicate differential expression induced by PFCAs or
210 NFCAs is predominantly specific to a particular phase of growth.

211 **Transcriptional response of mid-exponential *E. coli* to PFCAs**

212 Bacterial gene expression shifts significantly between exponential phase and stationary
213 phase, reflecting the transition from active growth and energy production towards stress-mitigation
214 and survival in resource-limited environments (48, 54). We hypothesize PFCAs would alter gene
215 expression differently during exponential phase and stationary phase. To better understand the
216 response of *E. coli* to PFCAs at each growth phase within the study's time course, we sought to
217 identify genes that were differentially expressed by PFOA and PFDoA (common responses) and
218 the genes only changed by one PFCA (specific responses), starting at mid-exponential phase (6
219 hr). Highlights of our results of the response of *E. coli* to PFCAs and NFCAs across the time
220 course, discussed below, are illustrated in Figure 5.

221 PFOA and PFDoA each induced differential expression of approximately 50 genes at 6 hr
222 (Figure 4 A; Table SI 3; Table SI 4). This is less than 2% of genes in the transcriptome, indicating
223 growth in the presence of PFCAs does not seem to have a major impact on gene expression of
224 mid-exponential *E. coli*. Only seven genes were differentially expressed by both PFCAs at 6 hr (SI
225 Figure 5 D). These genes, *nadA*, *msyB*, *hiuH*, *galS*, *adiY, yceK,* and *ymfQ,* encode a quinolinate
226 synthase, acidic protein, hydroxyisourate hydrolase, DNA-binding transcriptional dual regulator
227 and activator, and two uncharacterized proteins, respectively (Table SI 5). With roles in pyrimidine
228 and purine metabolism, quinolinate synthase and hydroxyisourate hydrolase were also
229 downregulated by PFOA and PFDoA at 24 hr, indicating a sustained effect on gene expression. As
230 an (4Fe-4S) cluster is required for activity of quinolinate synthase in NAD synthesis (55),
231 downregulation of *nadA* could suggest a requirement for iron and sulfur that correlates with
232 upregulation of sulfate assimilation and ferrous iron transport genes discussed in later sections.
233 The DNA-binding transcriptional dual regulator GalS was upregulated by PFOA at 6 hr, but
234 downregulated by PFDoA, suggesting *E. coli* exhibited a different response to the 8-chain PFCA
235 compared to the 12-chain. Several of these genes were also downregulated in response to the
236 NFCAs (Table SI 5; Table SI 7). For example, significant downregulation of *msyB* by both PFCAs
237 and NFCAs implies some changes in gene expression were not specific to fluorinated compounds,
238 but likely rather to carboxylic acids. The minimal common changes in gene expression at 6 hr
239 implies *E. coli* utilized different mechanisms at mid-exponential phase to respond to PFOA and
240 PFDoA.

241 During mid-exponential phase, *E. coli* differentially expressed several genes in response to
242 PFOA but not PFDoA, including the formate regulon, a putative transporter YhjX, L-aspartate
243 oxidase, L-alanine exporter, and small RNA RyjA (Table SI 3). Of particular interest, genes

244 encoding components of the formate regulon, including the formate hydrogenlyase (FHL)
245 complex, formate dehydrogenase H, and the hydrogenase pleiotropic *hyp* operon (56), were
246 significantly downregulated (Figure 5 A; Figure 6 A; Table SI 9). The FHL complex is essential to
247 fermentative H_2 production in *E. coli* during mixed-acid fermentation. At low extracellular pH and
248 high levels of re-imported formate during stationary phase, the FHL complex is activated to
249 disproportionate accumulated formate to hydrogen and carbon dioxide (57, 58). We found the
250 formate channel, encoded by *focA,* that transports formate from the cytoplasm during exponential
251 phase under physiological pH, was not differentially expressed at 6 hr by either PFCA or NFCA,
252 indicating these compounds did not induce more or less formate transport than the untreated
253 control. However, formate dehydrogenase H, encoded by *fdhF,* and the *hyc* operon, composed of
254 genes encoding the cytoplasmic domain subunits, *hycBEFG*, and membrane domains, *hycCD*, of
255 the FHL complex, plus the transcriptional regulator, *hycA*, chaperone, *hycH*, and protease, *hycI*,
256 were downregulated by PFOA at 6 hr (Figure 6 A; Table SI 9). Additionally, *hycBCDE* were also
257 significantly downregulated by PFOA at 48 hr, indicating the change in expression of these four
258 genes was not unique to mid-exponential phase. Four genes of the *hyp* operon, *hypABCD*, encoding
259 products involved in nickle:iron hydrogenase maturation (56, 59), and a gene encoding a putative
260 transporter predicted to function as an oxalate:formate antiporter, *yhjX* (60, 61), were also
261 downregulated at 6 hr by PFOA but not differentially expressed by PFDoA or either NFCA.
262 Downregulation of formate regulon genes, unfavorable reaction conditions in an aerobic
263 environment, and the unlikely occurrence of common inducing factors like acidic pH, the absence
264 of nitrates, and unlikely PFOA-induced formate accumulation during mid-exponential phase,
265 suggests forward conversion of formate was possibly prevented (57). These results further signify
266 a specific response to PFOA that differs from routine transport and conversion of formate under

267 physiological conditions. Lastly, formate is a degradation product of PFOA, and additional
268 measurements would be needed to determine if formate ions from PFOA were present in the
269 cultures.

270 During mid-exponential phase, PFDoA induced overexpression of genes involved in
271 sulfate and thiosulfate assimilation and L-cysteine biosynthesis (Figure 5 B, C; Figure 6 B; Table
272 SI 4; Table SI 10). Sulfate assimilation is crucial for the growth and survival of *E. coli*, as sulfur is
273 needed to synthesize cysteine and many cofactors and is important for cellular redox balance (62).
274 Sulfate and thiosulfate transporters are often overexpressed in *E. coli* when intracellular sulfur is
275 limited, and uptake of extracellular sulfate is needed (63). Newly assimilated sulfur-containing
276 intermediates are then converted to cysteine (64). The sulfate/thiosulfate ATP-binding cassette
277 (ABC) transporter complex, *cysPUWA,* was significantly upregulated with $\log_2$ fold changes
278 greater than 2.75 by PFDoA at 6 hr (Figure 6 B; Table SI 10). This was not observed with PFOA
279 or DoA. Genes encoding the transporter's periplasmic protein, *cysP*, and inner membrane subunit,
280 *cysU*, were also significantly upregulated by OA at 6 hr, indicating possible uptake of sulfate was
281 induced by OA as well (SI Figure 5 D). In a second path for sulfur assimilation, genes, *tsuAB*, in
282 a recently characterized thiosulfate ion uptake mechanism (65), were also upregulated by PFDoA
283 at 6 hr (Figure 6 B), but were not significantly changed by DoA. These results suggest PFDoA
284 induced a specific response to utilize this mechanism for thiosulfate ion uptake, and the response
285 was likely triggered by the 12-chain PFCA. Following sulfate and thiosulfate uptake, the genes
286 encoding enzymes that catalyze the activation and subsequent reduction of sulfate to intermediates,
287 sulfite and sulfide, were upregulated by PFDoA. The sulfate activation operon, *cysDNC*,
288 responsible for chemical activation of sulfate to adenosine 5'-phosphosulfate (APS) by ATP
289 sulfurylase and APS kinase and the gene cluster, *cysHIJ*, encoding APS reductase and sulfite

290 reductase subunits, responsible for the reduction of APS to sulfite and sulfite to sulfide (66, 67),
291 respectively, were overexpressed by PFDoA (Figure 6 B).

292 In addition to upregulation of sulfur-containing compound transporters and redox enzymes,
293 unsurprisingly, cysteine synthases, *cysKM* (64), and an inner membrane L-cystine (dimeric
294 cysteine) transporter, *tcyP*, were significantly upregulated by PFDoA at 6 hr (Figure 5 B; Figure 6
295 B). Furthermore, when grown on minimal medium, as done in this study, TcyP functions as the
296 main importer of L-cystine (68) and is activated when intracellular cysteine is low (64). These
297 changes in gene expression could indicate an increase requirement for cysteine through sulfate
298 assimilation or direct import in response to PFDoA. Lastly, the gene encoding the regulatory
299 protein CysB, which drives the sulfur limitation response in *E. coli,* was not differentially
300 expressed by any PFCA or NFCA treatment in this study (66, 69). It is possible the gene was
301 overexpressed at an early point in exponential phase as the genes it regulates were overexpressed
302 by PFDoA at the mid-exponential mark or has consistent expression. Overexpression of sulfate
303 and thiosulfate assimilation components and cysteine biosynthesis enzymes by PFDoA, indicates
304 PFDoA could be negatively impacting redox balancing and in turn, stimulating an increased
305 requirement for sulfur-containing compounds like cysteine during mid-exponential phase.

306 **Transcriptional response of early stationary phase *E. coli* to PFCAs**

307 During stationary phase, bacteria modulate gene expression by simultaneously activating
308 essential genes for survival and stress mitigation, while preventing transcription of unnecessary
309 genes in a nutrient-deficient environment. Additional stress induced by the prolonged presence of
310 PFCAs may further modify gene expression during stationary phase when compared to mid-
311 exponential phase. Unlike mid-exponential phase, the number of genes differentially expressed
312 specifically by PFOA or PFDoA during stationary phase at 24 hr was minimal (SI Figure 5 D, E).

313 PFOA induced specific changes in gene expression of genes encoding cytochrome bo3 subunits,
314 biotin biosynthesis enzymes, and transporters for iron and tryptophan (Table SI 3), whereas PFDoA
315 induced changes in gene expression of inner membrane proteins and the small regulatory RNA
316 GadY (Table SI 4). In contrast to minimal common responses observed at 6 hr, PFOA and PFDoA
317 induced differential expression of the same 49 genes at 24 hr (SI Figure 5 D, E, F; Table SI 5).
318 Products of these genes have roles in ferrous iron transport (Figure 7 A), amino acid metabolism
319 (Figure 7 B), and small RNA regulation (Figure 7 C). Common changes in gene expression suggest
320 these responses are not specific to a particular length of PFCAs, but to the PFCAs explored within
321 the scope of this study. Expression of 24 of the 49 genes were also significantly changed by OA at
322 24 hr and only 10 were changed by DoA (SI Figure 5 E; Table SI 5; Table SI 7), indicating those
323 genes likely have a larger role regarding carboxylic acids in general, rather than fluorination.

324 As iron is an essential nutrient and cofactor in various enzymes, several iron acquisition
325 systems and regulators have evolved to maintain intracellular iron homeostasis (70, 71). Our
326 analysis revealed genes encoding components of iron uptake transport mechanisms were
327 differentially expressed in response to PFCAs (Figure 5 D; Table SI 5; Table SI 11). One operon
328 *feoABC*, which encodes ferrous iron (Fe^{2+}) transporters (72), was significantly upregulated at 24
329 hr and 48 hr by both PFOA and PFDoA (Figure 7 A; SI Figure 5 F). The operon was also
330 upregulated at 24 hr by OA (Table SI 11), implying the elevated response could be stimulated by
331 the carboxylic acid moiety. Upregulation of *feo,* in combination with no significant change in the
332 expression of upstream Fur and Fnr transcripts, the ferric iron (Fe^{3+}) transcriptional regulator and
333 activator, (73, 74), suggests PFCAs induce a requirement for intracellular ferrous iron during
334 stationary phase. We hypothesize this is due to preference for the soluble ferrous form in
335 comparison to insoluble ferric form at the pH of the culture. Moreover, the level of free iron could

336 increase via *feo* transport because a putative Fur-regulated inhibitor, *rhyB,* (75, 76) was
337 downregulated by PFOA at 48 hr. Additionally, fluoride exposure can deplete active forms of metal
338 ions, including iron, through formation of stable metal-fluoride complexes, therefore, triggering
339 cells to increase free metal ion concentration (77, 78) to maintain homeostasis. Siderophores,
340 secreted ferric iron scavengers (79, 80), were not employed because the enterobactin gene cluster
341 and associated transporters were moderately downregulated at 48 hr by PFOA (Table SI 11).
342 However, genes, *exbB* and *exbD*, in the associated TonB energy-transducing complex (81) were
343 upregulated by PFOA and PFDoA at 48 hr (Figure 7 A). The *efeUOB* operon encoding a ferrous
344 iron transporter complex is not fully functional in *E. coli* MG1655 due to a frameshift mutation in
345 *efeU* (82), but the genes encoding periplasmic proteins*, efeO* and *efeB*, were also downregulated
346 by both PFCAs at 24 hr. Additionally, PFOA-induced downregulation of genes encoding various
347 cytochromes (Table SI 11) during stationary phase could suggest limited available iron for
348 incorporation into heme groups (83-85). These results further signify a specific preference and
349 need for ferrous iron uptake by the *feo* operon during stationary phase and likely limited
350 availability for incorporation in key components like cytochromes (84).

351 During stationary phase, gene expression is altered to meet metabolic requirements
352 including the adjustment of amino acid metabolism (86, 87). Genes encoding the *trp* operon, the
353 *thr* operon, isoleucine synthesis components (*ilvADE* and *ilvM*), and transporters of branched-
354 chain amino acids (*brnQ* and *livFGM*) were differentially expressed by PFOA and PFDoA during
355 stationary phase (Figure 5 E; Figure 7 B; Table SI 11). Notably, differences in gene expression
356 between PFCA samples and the untreated controls of the *trp* and *thr* operons were some of the
357 largest in this study, with $\log_2$ fold changes less than -5.3 and greater than 4.6, respectively.
358 Downregulation of the *trp* operon would suggest an effort to route metabolic flux towards optimal

359 parts of central metabolism or amino acid biosynthesis pathways (SI Figure 6) (88), in order to
360 adapt to high levels of intracellular tryptophan or related PFCA-induced stress. Alternatively,
361 upstream precursors to the *trp* operon, like chorismate (89), may not have been available, and as a
362 result, the operon was underexpressed. The *trp* operon was also downregulated by DoA at 6 hr and
363 OA at 24 hr (Figure 7 B; Table SI 11), indicating the change in gene expression was possibly
364 prompted by the octanoic acid moiety regardless of the presence or absence of fluorination.
365 Moreover, downregulation of tryptophan symporters, *mtr* and *tnaB*, at 24 hr and no change in
366 expression of the general aromatic acid transporter, *aroP*, imply extracellular tryptophan was likely
367 not imported into cell (Table SI 11). Upregulation of threonine and isoleucine biosynthesis genes
368 could be a direct result of carbon flux redirection from upper metabolism, and the synthesized
369 amino acids (90, 91) could be used in processes to mitigate stress and sustain growth during
370 nutrient-limited stationary phase.

371 Small regulatory RNAs (sRNAs) help modulate gene expression during stationary phase
372 and under environmental stress by stabilizing specific mRNAs and stimulating translation (92). At
373 24 hr, 10 sRNAs, their corresponding mRNAs targets, and flanking genes were downregulated by
374 PFOA and PFDoA (Figure 5 F; Figure 7 C; Table SI 11). A handful of these genes remained
375 downregulated by PFOA at 48 hr. In this study, this response was fairly specific to PFCAs, as only
376 four of these genes were differentially expressed by NFCAs. Also, the genes encoding RNA-
377 binding proteins Hfq and ProQ were minimally overexpressed by PFOA at 48 hr with $\log_2$ fold
378 changes of approximately one. These proteins work in tandem with sRNAs to bind target mRNAs
379 and provide intracellular stability (93). Downregulation of antisense sRNAs genes, *arrS* and *gadY*,
380 the corresponding mRNAs that they target, *gadE* and *gadX*, and flanking genes, *hdeAD, gadAFW,*
381 *and mdtF,* during stationary phase by PFOA and PFDoA (Figure 7 C), suggests possible energy

382 conservation and resource reallocation to critical survival pathways (92, 94) in response to PFCAs.
383 Lastly, *arrS* and *gadY* products have essential roles in acid resistance regulation (94), and
384 downregulation of these sRNAs at 24 hr suggests PFCAs either do not significantly induce acid
385 stress compared to the untreated control, or the activation of pH homeostasis mechanisms is too
386 costly due to nutrient limitation during stationary phase.

387 **Transcriptional response of late stationary phase *E. coli* to PFCAs**

388 To compare the transcriptional response of *E. coli* to PFCAs at different points within
389 stationary phase, we wanted to understand how differential expression patterns induced at 48 hr
390 differed from patterns at 24 hr. At 48 hr, PFOA and PFDoA upregulated 28 common genes that
391 encode the 50S ribosomal subunits, the DNA-binding transcriptional repressor LsrR, and Ton
392 complex subunit ExbD (Table SI 5; SI Figure 5 E, F). Seventeen of these genes were also
393 moderately upregulated by OA (Table SI 7), with a $\log_2$ fold change of at least 1.4, indicating
394 differential expression may not be specific to PFCAs. We observed specific changes in gene
395 expression of cold shock proteins and putative phosphotransferase system enzymes by PFDoA at
396 48 hr (Table SI 4).

397 In contrast to the minor response to PFDoA, PFOA induced the largest and broadest change
398 in gene expression in the entire study at 48 hr. For this timepoint, we observed a change in gene
399 expression of a fluoride exporter, central metabolism enzymes, ribosomal proteins, molecular
400 chaperones, autoinducer-2, and motility components induced by PFOA (Figure 8; SI Figure 6;
401 Table SI 3; Table SI 12; Table SI 13, Table SI 14).

402 High concentrations of environmental fluoride can inhibit metabolism, ribosomes, and
403 protein processing, in addition to altering pH and inducing oxidative stress in *E. coli* (45, 78).
404 Similar molecular mechanisms of oxidative stress along with membrane permeability have been

405 demonstrated by PFAS toxicity (38, 95, 96). Exporters, including the selective Fluc family fluoride
406 ion channels, mediate fluoride resistance and protect bacteria against toxicity (97). The *crcB* gene
407 of *E. coli* encodes a Fluc fluoride transport channel to expel fluoride out of the cell (45). Moderate
408 upregulation, $\log_2$ fold change of 1.4, of *crcB* at 48 hr by PFOA suggests a need to export
409 intracellular fluoride potentially accumulated from PFOA throughout the time course (Figure 5 G;
410 Figure 8 A; Table SI 12). Previous studies have observed the partitioning of PFAS with varying
411 chain length into bacterial membranes and subsequent increase in membrane fluidity (95, 96). In
412 addition, *E. coli* has mechanisms to indiscriminately uptake fluoride through membrane ion
413 channels or porins (45, 98). These results suggest a potential chain-length difference in PFCA
414 uptake and subsequent fluoride accumulation, as *crcB* was not differentially expressed by PFDoA
415 at 48 hr. Additional measurements will be needed to further explore this result.

416 Key components in various biological processes including glycolysis and the citric acid
417 cycle (TCA) enzymes, ribosomal proteins, ATPases, and molecular chaperones were also
418 upregulated at 48 hr by PFOA (Figure 8 A; Table SI 12). Vital for bacterial growth, genes encoding
419 glycolytic enzymes enolase, *eno*, and pyruvate kinases, *pykF* and *pykA*, were moderately
420 upregulated by PFOA at 48 hr (Figure 8 A; SI Figure 6), while *ppsA*, the phosphoenolpyruvate
421 (PEP) synthetase encoding gene, which catalyzes a reverse reaction from pyruvate to PEP, was not
422 differentially expressed. Enolase and kinases can be inhibited by micromolar amounts of fluoride
423 as the ion can complex to metal ion active sites displacing the electronegative substrate (97, 99).
424 Fluoride inhibition of the activity of these key enzymes in central metabolism can result in the
425 suspension of bacterial growth until fluoride is removed (45, 100). Upregulation of glycolytic
426 enzymes at 48 hr provides further evidence of a specific response to possible fluoride accumulation
427 from PFOA and export with *crcB*. Moreover, additional measurements within and beyond the time

428 course could show if *crcB* mediated export of fluoride alleviates possible inhibition. The *sucABCD*
429 operon, encoding TCA enzymes, was significantly upregulated by PFOA at 48 hr, whereas the
430 upstream *sdhCDAB* operon, encoding succinate dehydrogenase, was moderately upregulated, $\log_2$
431 fold change of approximately 1.0 and 1.2, by PFOA at PFDoA, respectively (Figure 8 A; SI Figure
432 6). Conversion of succinyl-CoA to succinate generates GTP indirectly contributing to energy
433 production (101). Succinyl-CoA also plays a role in peptidoglycan biosynthesis by generating
434 precursor lysine and diaminopimelate (102). Overexpression key metabolic enzymes and the
435 fluoride exporter at 48 hr, suggests *E. coli* could be recovering from possible fluoride inhibition
436 during stationary phase. In connection to partial upregulation of glycolytic and TCA enzymes,
437 genes encoding products of mixed-acid fermentation were also overexpressed in response to PFOA
438 at 48 hr (Figure 8 A; SI Figure 6). Upregulation of genes (*pta, ackA, poxB*, *adhE*) encoding
439 enzymes for pyruvate and acetyl-CoA conversion to acetate, succinate, and ethanol, in addition to
440 activation of upstream enolase further corroborates a possible restart of central metabolism (103).
441 Furthermore, production of mixed-acid fermentation products and TCA intermediates, implies an
442 essential metabolic requirement for survival in nutrient-limited stationary phase exacerbated by
443 PFOA.

444 Growth in the presence of PFCAs induced the overexpression of ribosomal proteins at 48
445 hr (Figure 5 H). Forty-two genes encoding 50S and 30S ribosomal protein subunits (104) were
446 upregulated by PFOA at 48 hr, and 17 of which were also upregulated by PFDoA (Table SI 12).
447 Though ribosome biogenesis can be reduced in response to nutrient limitations and stress (105),
448 and fluoride can inhibit protein synthesis (77), the observed increase in gene expression of
449 ribosomal proteins could suggest a requirement for machinery to translate new proteins in response
450 to PFCAs late in stationary phase. These results also suggest an increase in ribosome biogenesis

451 in response to the possible decrease in fluoride concentration by *crcB*-mediated export of fluoride.
452 This observation is corroborated by similar findings in a proteomics study of upregulation of
453 ribosomal proteins in anerobic *E. coli* supplemented with PFOA (38).

454 Several ATPases, including transporters and molecular chaperones, were also upregulated
455 by PFOA at 48 hr despite no significant change in expression at 24 (Figure 8 B; Table SI 12).
456 ATPases are integral to survival and stress adaptation, and PFCA-induced stress or inhibition by
457 fluoride (78, 106, 107) could lead to disruption of energy metabolism and cellular homeostasis.
458 Upregulation of the ATP-dependent Lon protease (Figure 8 B), with roles in metabolic regulation,
459 protein quality control, and degradation of abundant ribosomal proteins (108, 109), at 48 hr,
460 implies a possible need for the protease to degrade misfolded or abnormal proteins to supply amino
461 acids for protein synthesis during stationary phase (110). Gene expression of ABC transporter
462 ATPases in the oligopeptide transport system, *oppD* and *oppF,* and maltose transport, *malK*, (111)
463 varied throughout the time course. Initially, the ATPases were upregulated at 6 hr, not differentially
464 expressed at 24 hr, and moderately upregulated again at 48 hr by PFOA (Figure 8 B). Likewise, a
465 proteomics study found upregulation of the same oligopeptide-binding proteins in *E. coli*
466 cultivated with PFOA (38). The gene encoding the ATPase SecA and other essential components
467 of the bacterial Sec translocase, *secYG*, (112, 113), were also upregulated at 48 hr (Figure 8 B;
468 Table SI 12). As protein secretion is essential in bacteria, the Sec system provides a form of
469 transmembrane translocation to ferry polypeptides from the cytoplasm across the cytoplasmic
470 membrane into the periplasm (114, 115). Overexpression of these genes suggests possible PFOA-
471 induced intracellular protein accumulation and likely saturation of existing Sec-translocases at 48
472 hr. Moreover, if fluoride possibly inhibited SecA, upregulation at 48 hr implies an increased
473 abundance of SecA transcripts, similar to other ATPases discussed. Although the gene encoding

474 SecB, the protein secretion chaperone that interacts with the Sec translocase, was not even
475 moderately upregulated with a $\log_2$ fold change of 0.81, other molecular chaperones may assist in
476 protein processing in response to PFOA.

477 Bacteria employ molecular chaperones as regulators and facilitators of protein folding,
478 transport, and control to maintain cellular homeostasis, especially during environmental stress.
479 ATP-dependent molecular chaperones DnaK, GroEL, and trigger factor (TF) along with
480 cochaperones DnaJ, GrpE, and GroES coordinate the folding of newly synthesized cytosolic
481 proteins in *E. coli* (116). Genes encoding the chaperone network, *dnaKJ, groLS*, *clpB,* and *htpG*,
482 were highly overexpressed by PFOA at 48 hr (Figure 5 I; Figure 8 B; Table SI 12). Conversely, the
483 genes were initially downregulated by PFOA at 6 hr. Molecular chaperones are overexpressed in
484 response to other environmental stressors such as temperature, heavy metals, limited nutrients, and
485 chemical pollutants (117, 118). Upregulation of molecular chaperones genes during stationary
486 phase suggests stress-induced activation in reaction to the presence of PFOA. This is consistent
487 with existing literature that has found PFAS can destabilize and denature proteins (119, 120).
488 Although PFDoA induced moderate overexpression of select chaperones at 48 hr (Figure 8 B),
489 significant upregulation by PFOA of the chaperone network indicates a chain-length dependent
490 response. Moreover, these results also suggest a specific response to PFCAs as there was no
491 significant change in gene expression induced by either NFCA at 48 hr.

492 Further analysis revealed PFOA triggered various stress responses as genes encoding sigma
493 factors, components of envelope stress response mechanisms, and motility systems of flagellar
494 assembly and chemotaxis were differentially expressed (Figure 8 C, D; SI Figure 7). RNA
495 polymerase (RNAP) core enzyme subunits, *rpoA and rpoBC*, RNAP sigma factors, *rpoE, rpoH,*
496 *rpoF/fliA,* and *rpoS,* and RpoE regulators, *rseABC,* were highly upregulated by PFOA and only

497 moderately upregulated by OA at 48 hr (Figure 8 C; Table SI 13). As these genes have regulatory
498 roles in the transcription of genes involved in outer membrane stress response, heat shock, flagellar
499 assembly, and stationary phase gene expression, respectively, overexpression suggests heightened
500 regulation of mechanisms employed to mitigate possible stress of PFCAs and NFCAs (121-123).
501 Similar to RNAP and sigma factors, the phage-shock-protein (Psp) operon, *pspABCD*, was also
502 upregulated by PFOA and OA at 48 hr (Figure 8 C; Table SI 13). In contrast to OA, the magnitude
503 of overexpression of the operon by PFOA increased over the time course. As the Psp system can
504 be initiated by a damaged inner membrane (124) and Sec translocase overload (125), an increase
505 in expression throughout the time course by PFOA suggests use of the regulation mechanism to
506 combat possible envelope stress. Our results show additional evidence of PFOA-induced envelope
507 stress as the lipopolysaccharide (LPS) gene clusters responsible for the synthesis of the core
508 oligosaccharide structure, *rfa*, and the lipid A soluble proteins, *lpxA, lpxC,* and *lpxD*, and the ATP-
509 binding LPS transporter, *msbA,* (126) were moderately upregulated at 48 hr (Figure 8 C; Table SI
510 13). Overexpression of these genes may suggest the need to synthesize LPS components to
511 maintain the outer membrane, despite the high energetic cost. Previous studies have shown that
512 PFAS partition into lipid bilayers and disrupt bacterial membranes, leading to increased
513 permeability (95, 96, 127). Our results suggest *E. coli* is employing several mechanisms to mitigate
514 envelope stress, likely from PFOA.

515 To adapt to limited resources in stationary phase and respond to external stressors, bacteria
516 will downregulate high energetic-cost processes like motility to reallocate resources to survival
517 (128, 129). We observed downregulation of genes encoding components involved in flagellar
518 assembly, chemotaxis, and extracellular polysaccharide biosynthesis (EPS) at 48 hr by PFOA
519 (Figure 5 J; Figure 8 D; SI Figure 7; Table SI 14). These results suggest PFOA could be inducing

520 a transition from a sessile state towards possible biofilm formation, therefore reducing motility via
521 downregulation of flagellar assembly, as an indirect effect, in order to conserve energetic
522 resources. Notably, DoA-induced upregulation of the same flagellar assembly and chemotaxis
523 genes during mid-exponential phase (SI Figure 7; Table SI 14) suggests these processes may have
524 been used to respond to DoA and to follow nutrient gradients. Moreover, these genes were not
525 significantly changed by OA or PFDoA at any point in the time course, suggesting a specific
526 response to PFOA at 48 hr. Furthermore, genes encoding autoinducer-2 (AI-2), *luxS*, a quorum-
527 sensing (QS) molecule (130) and the ABC transporter *lsr* operon, used for AI-2 uptake, were
528 significantly upregulated by PFOA at 48 hr (Figure 8 D; Table SI 14). AI-2 controls gene
529 expression of chemotaxis and flagellar assembly and has a possible link to biofilm formation (131).
530 A previous study found PFAS induced the production of EPS, biofilm precursor, in *Rhodococcus*
531 as a stress response (132). Although EPS biosynthesis genes are downregulated at 48 hr, with the
532 exception of the *rfb* operon (Table SI 14), additional measurements after 48 hr could provide
533 insight into possible PFOA-induced biofilm formation.

534 **CONCLUSIONS**

535 In summary, we performed time course RNA-seq to characterize the transcriptional
536 responses of mid-exponential phase and stationary phase *E. coli* to PFCAs, PFOA and PFDoA.
537 Our results suggest 100 μmol/L of either PFCA or respective NFCAs do not statistically impact
538 the growth of *E. coli* at any point in the time course relative to the untreated control. However,
539 differential expression analysis revealed PFOA and PFDoA did induce statistically significant
540 changes in gene expression of the formate regulon and sulfate assimilation at mid-exponential
541 phase and ferrous iron transport, the molecular chaperone network, and motility processes during
542 stationary phase. The time course enabled us to capture the specific and common responses of *E.*

543 *coli* to PFCAs and NFCAs across time and helped to characterize responses that were specific to
544 a single growth phase or prolonged over time. For instance, our results indicate a requirement for
545 sulfur-containing compounds, like cysteine, during mid-exponential phase as sulfate assimilation
546 components were overexpressed in response specifically to PFDoA. In contrast, overexpression of
547 ferrous iron transporters and amino acid enzymes by PFOA and PFDoA early in stationary phase
548 suggest a time dependent need for ferrous iron and select amino acids. Although differentially
549 expressed at different phases within the time course, sulfur-containing compounds and iron
550 participate in various redox reactions within the cell which could suggest PFCAs induce
551 adjustments to cellular redox. Interestingly, PFOA induced the largest change in gene expression
552 of this study at 48 hr, whereas PFDoA induced a minor change in expression. These results suggest
553 different modes of interactions between *E. coli* and two PFCAs that only differ in length by four
554 carbons but have different physiochemical properties.

555 These results not only provide additional biological context of the response of *E. coli* to
556 PFCAs at key phases of growth, but possible novel engineering targets to facilitate the
557 development of future environmental monitoring and mitigation strategies. For example, gene
558 expression of numerous small regulatory RNAs and their targets was only significantly changed
559 by PFCAs and not by NFCAs (Figure 7 C), suggesting a unique response to fluorinated compounds
560 that could be utilized in a whole cell biosensor. Additionally, the moderate upregulation of *crcB*, a
561 putative fluoride exporter downstream of a fluoride riboswitch, by PFOA at 48 hr (Figure 8 A),
562 suggests there may have been some removal of fluorine from the PFOA over the time course,
563 warranting further investigation as a mitigation strategy.

564 Even though these measurements offer a comprehensive transcriptomic snapshot of the
565 relationship between PFCAs and a model bacterium at key growth phases, further characterization

566 efforts would benefit from additional measurements of PFAS with different molecular structures,
567 concentrations, and complex mixtures to explore the extent to which the responses identified here
568 are conserved and identify novel responses. Furthermore, conducting similar studies on
569 environmental microorganisms and microbial communities could provide insight into conserved
570 responses across genera and species and how contamination by PFAS impacts the environment.
571 As technology continues to advance, improved gene expression measurements at the single cell,
572 population, and community level combined with multiomics level analysis would enable more
573 accurate, impactful understanding of PFAS at all levels of biology. This complete picture could aid
574 in the rapid development of inexpensive and easy-to-deploy living measurement systems for *in*
575 *situ* environmental monitoring and mitigation strategies.

576 **MATERIALS AND METHODS**

577 **Bacterial strain**

578 *Escherichia coli* MG1655 ATCC 47076 was obtained from the American Type Culture
579 Collection (ATCC). The strain was maintained on Luria-Bertani (LB) agar plates at 37 °C prior to
580 use.

581 **PFOA, PFDoA, and NFCA preparation**

582 Two PFCAs, perfluorooctanoic acid (96%, PFOA) and tricosafluorododecanoic acid (95%,
583 perfluorododecanoic acid, PFDoA) were used in this study. See Table SI 15 for additional chemical
584 stock information. PFOA and PFDoA were dissolved in dimethyl sulfoxide (DMSO) to prepare a
585 stock solution of 100 mmol/L. Concentrations in the growth medium for growth experiments were
586 100 μmol/L and 10 100 μmol/L. The final concentration in the growth medium for sequencing
587 experiments was 100 μmol/L. DMSO was present in the growth medium at a final volume fraction
588 of 0.1%. Dodecanoic acid (98%, DoA) was prepared in the same way as the PFCA stocks. Octanoic
589 acid (99%, OA) samples contained an addition of DMSO to the growth medium. All untreated
590 samples contained an equivalent concentration of DMSO and were devoid of PFCA addition.

591 ***E. coli* growth in PFCA or NFCA containing medium**

592 *E. coli* MG1655 was struck onto an LB agar (BD Difco) plate from a glycerol stock
593 obtained from ATCC. Overnight cultures for each biological replicate were prepared by
594 inoculating 3 mL of M9 minimal medium (133), without PFCA or NFCA addition, with an
595 individual colony incubated at 37 °C, 250 rpm (Table SI 15). For flask-based growth experiments,
596 PFCA stocks, NFCA stocks, or DMSO were added into M9 prior inoculation with *E. coli* cultures
597 as described above. To prepare sample flasks, 50 mL of M9 in sterile 125 mL baffled flasks was
598 inoculated with overnight culture and adjusted to a starting optical density at 600 nm of 0.01 (SI

599 Figure 1; Table SI 1). Cultures were incubated at 37 °C, 250 rpm for 48 hr. Independent biological
600 triplicate flasks were used for each PFCA, NFCA, and untreated control group. To obtain the
601 optical density of each culture, bacterial growth was monitored in each culture with absorbance
602 measurements at 600 nm in technical triplicate throughout the 48 hr period. A Biotek Epoch2
603 microplate reader was used for absorbance measurements. A two-way mixed ANOVA of optical
604 density measurements was performed in RStudio running R version 4.2.2 with functions from
605 packages tidyverse (v2.0.0) and rstatix (v0.7.2) (134, 135).

606 **Total RNA Extraction, cDNA Library preparation, and RNA Sequencing**

607 Cell pellets of *E. coli* from each sample type (PFCA, NFCA, or untreated control) were
608 harvested at 6 hr, 24 hr, and 48 hr and normalized to an OD_{600} of 1.0. Samples were spun down at
609 5,500xg for 7 min at 4 °C, and supernatant was removed prior to storage at -80 °C until total RNA
610 extraction.

611 Total RNA was extracted from biological triplicates of each PFCA, NFCA, and untreated
612 control at 6 hr, 24 hr, and 48 hr using RNeasy Mini Kit (Qiagen) according to the manufacturer's
613 instructions with an on-column DNase I digestion for 15 min using an RNase-free DNase Set
614 (Qiagen). Cells were lysed in 200 µL Tris-EDTA buffer solution, pH 8.0 containing 20 g/L
615 lysozyme (Sigma Aldrich) at room temperature for 10 min with vortexing every 2 min. RNA was
616 eluted in 35 µL of molecular grade water (Invitrogen) and stored at -80 °C. The concentration and
617 purity of total RNA were quantified on a Qubit 4 fluorometer (Invitrogen) using Qubit RNA Broad
618 Range Assay Kit, DeNovix D-11 Series Spectrophotometer, and 4200 TapeStation System
619 (Agilent) using RNA ScreenTape Analysis.

620 Total RNA samples were sent to Azenta Life Sciences (USA) for cDNA library preparation
621 using TruSeq Stranded mRNA kit (Illumina) and next-generation sequencing (Strand-Specific

622 RNA-Seq Service) using an Illumina HiSeq platform for 2x150 bp paired-end reads. Average
623 sequencing depth obtained was 7.81 million. Additional information on sequencing is provided in
624 (Table SI 2).

625 **Bioinformatic analysis**

626 Bioinformatic analysis was performed on an Amazon Web Service EC2 instance and
627 locally on RStudio. TrimGalore (v0.6.7) with Cutadapt (v3.5) and fastQC (v0.11.9) was used to
628 remove adapter sequences and low-quality reads from each raw read file (136-138). HISAT2
629 (v2.2.1) (139) was used to align paired-end reads to *E. coli* MG1655 reference genome (GenBank
630 accession GCA_000005845.2). Alignment scores and quality metric scores are shown in Table SI
631 2. Samtools (v1.13) was used for file conversion of SAM files to sorted BAM files before transcript
632 assembly was performed with Stringtie (v2.2.1) (140, 141). In RStudio running R version 4.2.2,
633 tximport (v1.26.1) prepared count tables from Stringtie transcript-level estimates (134, 135, 142).
634 DESeq2 (v1.38.3) was used to perform differential gene expression analysis with a negative
635 binomial distribution model (49). The time specific untreated control served as the control baseline
636 for all pairwise comparisons. In this study, we consider genes to be differentially expressed if the
637 Benjamini-Hochberg adjusted p-value (padj) is less than 0.05. We mark moderate and significant
638 differential expression with absolute values of the $\log_2$ fold change greater than or equal to 1.2 and
639 1.5, respectively. Gene ontology and Kyoto Encyclopedia of Genes and Genomes pathway over-
640 representation analyses were performed using clusterProfiler (v4.6.2) using the *E. coli* K12
641 organism package, org.EcK12.eg.db, (v3.19.1) and KEGG organism eco (143, 144). Additional
642 data curation was performed using EcoCyc (145).

643

644

DATA AVAILABILITY

The data presented in this study have been deposited in the National Center for Biotechnology Information's Gene Expression Omnibus (146) and are accessible through GEO Series accession number GSE288896 (https://www.ncbi.nlm.nih.gov/geo/query/acc.cgi?acc=GSE288896).

ACKNOWLEDGEMENTS

Author contributions: M.E.W. conceived the project, designed experiments, conducted data analysis, and wrote the first draft with input from S.W.S. O.B.V. designed growth experiments. M.E.W. and S.W.S edited the manuscript with input from all authors.

The authors would like to thank Elizabeth Strychalski, Allison Yaguchi, Justin Wagner, Svetlana Ikonomova, and Zoila Jurado Quiroga for insightful discussions throughout the project and on the manuscript.

Figure 1, Figure 5, SI Figure 1, and SI Figure 6 were created with BioRender.com.

Disclaimer: Certain commercial entities, equipment, or materials may be identified in this document to describe an experimental procedure or concept adequately. Such identification is not intended to imply recommendation or endorsement by the National Institute of Standards and Technology, nor is it intended to imply that the entities, materials, or equipment are necessarily the best available for the purpose. Official contribution of the National Institute of Standards and Technology; not subject to copyright in the United States.

FUNDING

This work was supported by a National Research Council Postdoctoral Fellowship to M.E.W.

REFERENCES

1. Parsons JR, Sáez M, Dolfing J, de Voogt P. 2008. Biodegradation of perfluorinated compounds. Rev Environ Contam Toxicol 196:53-71.
2. Glüge J, Scheringer M, Cousins IT, DeWitt JC, Goldenman G, Herzke D, Lohmann R, Ng CA, Trier X, Wang Z. 2020. An overview of the uses of per- and polyfluoroalkyl substances (PFAS). Environ Sci Process Impacts 22:2345-2373.
3. Williams AJ, Gaines LGT, Grulke CM, Lowe CN, Sinclair GFB, Samano V, Thillainadarajah I, Meyer B, Patlewicz G, Richard AM. 2022. Assembly and Curation of Lists of Per- and Polyfluoroalkyl Substances (PFAS) to Support Environmental Science Research. Front Environ Sci 10:1-13.
4. Faust JA. 2023. PFAS on atmospheric aerosol particles: a review. Environ Sci Process Impacts 25:133-150.
5. Abunada Z, Alazaiza MYD, Bashir MJK. 2020. An overview of per- and polyfluoroalkyl substances (PFAS) in the environment: source, fate, risk and regulations. Water 12.
6. LaKind JS, Naiman J, Verner MA, Lévêque L, Fenton S. 2023. Per- and polyfluoroalkyl substances (PFAS) in breast milk and infant formula: A global issue. Environ Res 219:115042.
7. Graber JM, Alexander C, Laumbach RJ, Black K, Strickland PO, Georgopoulos PG, Marshall EG, Shendell DG, Alderson D, Mi Z, Mascari M, Weisel CP. 2019. Per and polyfluoroalkyl substances (PFAS) blood levels after contamination of a community water supply and comparison with 2013-2014 NHANES. J Expo Sci Environ Epidemiol 29:172-182.
8. Li J, Sun J, Li P. 2022. Exposure routes, bioaccumulation and toxic effects of per- and polyfluoroalkyl substances (PFASs) on plants: A critical review. Environ Int 158:106891.
9. Piva E, Giorgetti A, Ioime P, Morini L, Freni F, Faro FL, Pirani F, Montisci M, Fais P, Pascali JP. 2021. Hair determination of per- and polyfluoroalkyl substances (PFAS) in the Italian population. Toxicology 458:152849.
10. Brusseau ML, Anderson RH, Guo B. 2020. PFAS concentrations in soils: Background levels versus contaminated sites. Sci Total Environ 740:140017.
11. Coperchini F, Croce L, Ricci G, Magri F, Rotondi M, Imbriani M, Chiovato L. 2020. Thyroid Disrupting Effects of Old and New Generation PFAS. Front Endocrinol (Lausanne) 11:612320.
12. Evich MG, Davis MJB, McCord JP, Acrey B, Awkerman JA, Knappe DRU, Lindstrom AB, Speth TF, Tebes-Stevens C, Strynar MJ, Wang Z, Weber EJ, Henderson WM, Washington JW. 2022. Per- and polyfluoroalkyl substances in the environment. Science 375:eabg9065.
13. Zhang X, Zhao L, Ducatman A, Deng C, von Stackelberg KE, Danford CJ. 2023. Association of per- and polyfluoroalkyl substance exposure with fatty liver disease risk in US adults. JHEP Rep 5:100694.
14. Khan EA, Zhang X, Hanna EM, Yadetie F, Jonassen I, Goksøyr A, Arukwe A. 2021. Application of quantitative transcriptomics in evaluating the ex vivo effects of per- and polyfluoroalkyl substances on Atlantic cod (Gadus morhua) ovarian physiology. Sci Total Environ 755:142904.
15. USEPA. 2022. CompTox chemicals dashboard, PFAS master list of PFAS substances.

16. OECD H. 2021. Reconciling terminology of the universe of per-and polyfluoroalkyl substances: recommendations and practical guidance, vol 61, p 45. OECD Publishing Paris.
17. Buck RC, Franklin J, Berger U, Conder JM, Cousins IT, de Voogt P, Jensen AA, Kannan K, Mabury SA, van Leeuwen SP. 2011. Perfluoroalkyl and polyfluoroalkyl substances in the environment: terminology, classification, and origins. Integr Environ Assess Manag 7:513-41.
18. Berhanu A, Mutanda I, Taolin J, Qaria MA, Yang B, Zhu D. 2023. A review of microbial degradation of per- and polyfluoroalkyl substances (PFAS): Biotransformation routes and enzymes. Sci Total Environ 859:160010.
19. Weiner B, Yeung LWY, Marchington EB, D'Agostino LA, Mabury SA. 2013. Organic fluorine content in aqueous film forming foams (AFFFs) and biodegradation of the foam component 6 : 2 fluorotelomermercaptoalkylamido sulfonate (6 : 2 FTSAS). Environmental Chemistry 10:486-493.
20. Gonda N, Zhang C, Tepedelen D, Smith A, Schaefer C, Higgins CP. 2024. Quantitative assessment of poly- and perfluoroalkyl substances (PFASs) in aqueous film forming foam (AFFF)-impacted soils: a comparison of analytical protocols. Anal Bioanal Chem doi:10.1007/s00216-024-05585-2.
21. Lopez-Vazquez J, Montes R, Rodil R, Cela R, Martinez-Pontevedra JA, Pena MT, Quintana JB. 2024. Determination of regulated perfluoroalkyl substances (PFAS) in drinking water according to Directive 2020/2184/EU. Environ Sci Pollut Res Int doi:10.1007/s11356-024-34852-z.
22. USEPA. 2024. PFAS Analytical Methods Development and Sampling Research. https://www.epa.gov/water-research/pfas-analytical-methods-development-and-sampling-research. Accessed
23. Malouchi N, Chatzimichailidou S, Tolkou AK, Kyzas GZ, Calgaro L, Marcomini A, Katsoyiannis IA. 2024. The Removal of Per- and Poly-Fluoroalkyl Substances from Water: A Review on Destructive and Non-Destructive Methods. Separations 11:122.
24. Mahinroosta R, Senevirathna L. 2020. A review of the emerging treatment technologies for PFAS contaminated soils. Journal of Environmental Management 255:109896.
25. Stockbridge RB, Wackett LP. 2024. The link between ancient microbial fluoride resistance mechanisms and bioengineering organofluorine degradation or synthesis. Nat Commun 15:4593.
26. Cordner A, Goldenman G, Birnbaum LS, Brown P, Miller MF, Mueller R, Patton S, Salvatore DH, Trasande L. 2021. The True Cost of PFAS and the Benefits of Acting Now. Environ Sci Technol 55:9630-9633.
27. Sharma N, Kumar V, Sugumar V, Umesh M, Sondhi S, Chakraborty P, Kaur K, Thomas J, Kamaraj C, Maitra SS. 2024. A comprehensive review on the need for integrated strategies and process modifications for per- and polyfluoroalkyl substances (PFAS) removal: Current insights and future prospects. Case Studies in Chemical and Environmental Engineering 9:100623.
28. Mann MM, Berger BW. 2023. A genetically-encoded biosensor for direct detection of perfluorooctanoic acid. Scientific Reports 13:15186.
29. Thompson D, Zolfigol N, Xia Z, Lei Y. 2024. Recent progress in per- and polyfluoroalkyl substances (PFAS) sensing: A critical mini-review. Sensors and Actuators Reports 7:100189.

30. Tang Z, Vogel TM, Wang Q, Wei C, Ali M, Song X. 2024. Microbial defluorination of TFA, PFOA, and HFPO-DA by a native microbial consortium under anoxic conditions. Journal of Hazardous Materials 465:133217.
31. Griebler C, Lueders T. 2009. Microbial biodiversity in groundwater ecosystems. Freshwater Biology 54:649-677.
32. Jagevall S, Rabe L, Pedersen K. 2011. Abundance and diversity of biofilms in natural and artificial aquifers of the Aspo Hard Rock Laboratory, Sweden. Microb Ecol 61:410-22.
33. Nguyen J, Lara-Gutiérrez J, Stocker R. 2021. Environmental fluctuations and their effects on microbial communities, populations and individuals. FEMS Microbiol Rev 45.
34. Norman TM, Lord ND, Paulsson J, Losick R. 2015. Stochastic Switching of Cell Fate in Microbes. Annu Rev Microbiol 69:381-403.
35. Beale DJ, Sinclair GM, Shah R, Paten AM, Kumar A, Long SM, Vardy S, Jones OAH. 2022. A review of omics-based PFAS exposure studies reveals common biochemical response pathways. Science of The Total Environment 845:157255.
36. Reardon AJF, Rowan-Carroll A, Ferguson SS, Leingartner K, Gagne R, Kuo B, Williams A, Lorusso L, Bourdon-Lacombe JA, Carrier R, Moffat I, Yauk CL, Atlas E. 2021. Potency Ranking of Per- and Polyfluoroalkyl Substances Using High-Throughput Transcriptomic Analysis of Human Liver Spheroids. Toxicol Sci 184:154-169.
37. Rericha Y, St Mary L, Truong L, McClure R, Martin JK, Leonard SW, Thunga P, Simonich MT, Waters KM, Field JA, Tanguay RL. 2024. Diverse PFAS produce unique transcriptomic changes linked to developmental toxicity in zebrafish. Front Toxicol 6:1425537.
38. Yang M, Ye J, Qin H, Long Y, Li Y. 2017. Influence of perfluorooctanoic acid on proteomic expression and cell membrane fatty acid of Escherichia coli. Environ Pollut 220:532-539.
39. Bhatia RP, Kirit HA, Predeus AV, Bollback JP. 2022. Transcriptomic profiling of Escherichia coli K-12 in response to a compendium of stressors. Sci Rep 12:8788.
40. Wintenberg M, Manglass L, Martinez NE, Blenner M. 2023. Global Transcriptional Response of Escherichia coli Exposed In Situ to Different Low-Dose Ionizing Radiation Sources. mSystems 8:e0071822.
41. Valat C, Hirchaud E, Drapeau A, Touzain F, de Boisseson C, Haenni M, Blanchard Y, Madec JY. 2020. Overall changes in the transcriptome of Escherichia coli O26:H11 induced by a subinhibitory concentration of ciprofloxacin. Journal of Applied Microbiology 129:1577-1588.
42. Spiteri D, Griffin S, Karatzas KA, Scerri C, Valdramidis VP. 2023. Escherichia coli K-12 Transcriptomics for Assessing the Mechanism of Action of High-Power Ultrasound. Microorganisms 11.
43. Zango ZU, Ethiraj B, Al-Mubaddel FS, Alam MM, Lawal MA, Kadir HA, Khoo KS, Garba ZN, Usman F, Zango MU, Lim JW. 2023. An overview on human exposure, toxicity, solid-phase microextraction and adsorptive removal of perfluoroalkyl carboxylic acids (PFCAs) from water matrices. Environ Res 231:116102.
44. Addicks GC, Rowan-Carroll A, Reardon AJF, Leingartner K, Williams A, Meier MJ, Moffat I, Carrier R, Lorusso L, Wetmore BA, Yauk CL, Atlas E. 2023. Per- and polyfluoroalkyl substances (PFAS) in mixtures show additive effects on transcriptomic points of departure in human liver spheroids. Toxicol Sci 194:38-52.

45. Ji C, Stockbridge RB, Miller C. 2014. Bacterial fluoride resistance, Fluc channels, and the weak acid accumulation effect. J Gen Physiol 144:257-61.
46. Adamek E, Pawłowska-Góral K, Bober K. 2005. In vitro and in vivo effects of fluoride ions on enzyme activity. Ann Acad Med Stetin 51:69-85.
47. Breaker RR. 2012. New insight on the response of bacteria to fluoride. Caries Res 46:78-81.
48. Ishihama A. 1997. Adaptation of gene expression in stationary phase bacteria. Curr Opin Genet Dev 7:582-8.
49. Love MI, Huber W, Anders S. 2014. Moderated estimation of fold change and dispersion for RNA-seq data with DESeq2. Genome Biol 15:550.
50. Nobelmann B, Lengeler JW. 1996. Molecular analysis of the gat genes from Escherichia coli and of their roles in galactitol transport and metabolism. J Bacteriol 178:6790-5.
51. Ehrmann M, Boos W, Ormseth E, Schweizer H, Larson TJ. 1987. Divergent transcription of the sn-glycerol-3-phosphate active transport (glpT) and anaerobic sn-glycerol-3-phosphate dehydrogenase (glpA glpC glpB) genes of Escherichia coli K-12. J Bacteriol 169:526-32.
52. Gerike U, Hough DW, Russell NJ, Dyall-Smith ML, Danson MJ. 1998. Citrate synthase and 2-methylcitrate synthase: structural, functional and evolutionary relationships. Microbiology (Reading) 144 (Pt 4):929-935.
53. Yamanaka Y, Oshima T, Ishihama A, Yamamoto K. 2014. Characterization of the YdeO regulon in Escherichia coli. PLoS One 9:e111962.
54. Navarro Llorens JM, Tormo A, Martínez-García E. 2010. Stationary phase in gram-negative bacteria. FEMS Microbiol Rev 34:476-95.
55. Ollagnier-de Choudens S, Loiseau L, Sanakis Y, Barras F, Fontecave M. 2005. Quinolinate synthetase, an iron-sulfur enzyme in NAD biosynthesis. FEBS Lett 579:3737-43.
56. Skibinski DA, Golby P, Chang YS, Sargent F, Hoffman R, Harper R, Guest JR, Attwood MM, Berks BC, Andrews SC. 2002. Regulation of the hydrogenase-4 operon of Escherichia coli by the sigma(54)-dependent transcriptional activators FhlA and HyfR. J Bacteriol 184:6642-53.
57. Pinske C, Sargent F. 2016. Exploring the directionality of Escherichia coli formate hydrogenlyase: a membrane-bound enzyme capable of fixing carbon dioxide to organic acid. Microbiologyopen 5:721-737.
58. McDowall JS, Murphy BJ, Haumann M, Palmer T, Armstrong FA, Sargent F. 2014. Bacterial formate hydrogenlyase complex. Proc Natl Acad Sci U S A 111:E3948-56.
59. Lutz S, Jacobi A, Schlensog V, Böhm R, Sawers G, Böck A. 1991. Molecular characterization of an operon (hyp) necessary for the activity of the three hydrogenase isoenzymes in Escherichia coli. Mol Microbiol 5:123-35.
60. Pao SS, Paulsen IT, Saier MH. 1998. Major facilitator superfamily. Microbiol Mol Biol Rev 62:1-34.
61. Saier MH, Reddy VS, Moreno-Hagelsieb G, Hendargo KJ, Zhang Y, Iddamsetty V, Lam KJK, Tian N, Russum S, Wang J, Medrano-Soto A. 2021. The Transporter Classification Database (TCDB): 2021 update. Nucleic Acids Res 49:D461-D467.
62. Tanaka Y, Yoshikaie K, Takeuchi A, Ichikawa M, Mori T, Uchino S, Sugano Y, Hakoshima T, Takagi H, Nonaka G, Tsukazaki T. 2020. Crystal structure of a YeeE/YedE family protein engaged in thiosulfate uptake. Sci Adv 6:eaba7637.

63. Sirko A, Hryniewicz M, Hulanicka D, Böck A. 1990. Sulfate and thiosulfate transport in Escherichia coli K-12: nucleotide sequence and expression of the cysTWAM gene cluster. J Bacteriol 172:3351-7.
64. Imlay KRC, Korshunov S, Imlay JA. 2015. Physiological Roles and Adverse Effects of the Two Cystine Importers of Escherichia coli. J Bacteriol 197:3629-44.
65. Ikei M, Miyazaki R, Monden K, Naito Y, Takeuchi A, Takahashi YS, Tanaka Y, Murata K, Mori T, Ichikawa M, Tsukazaki T. 2024. YeeD is an essential partner for YeeE-mediated thiosulfate uptake in bacteria and regulates thiosulfate ion decomposition. PLoS Biol 22:e3002601.
66. Leyh TS, Vogt TF, Suo Y. 1992. The DNA sequence of the sulfate activation locus from Escherichia coli K-12. J Biol Chem 267:10405-10.
67. Leyh TS, Taylor JC, Markham GD. 1988. The sulfate activation locus of Escherichia coli K12: cloning, genetic, and enzymatic characterization. J Biol Chem 263:2409-16.
68. Deutch CE, Spahija I, Wagner CE. 2014. Susceptibility of Escherichia coli to the toxic L-proline analogue L-selenaproline is dependent on two L-cystine transport systems. J Appl Microbiol 117:1487-99.
69. Kredich NM. 1992. The molecular basis for positive regulation of cys promoters in Salmonella typhimurium and Escherichia coli. Mol Microbiol 6:2747-53.
70. Andrews SC, Robinson AK, Rodriguez-Quinones F. 2003. Bacterial iron homeostasis. FEMS Microbiol Rev 27:215-37.
71. McHugh JP, Rodriguez-Quinones F, Abdul-Tehrani H, Svistunenko DA, Poole RK, Cooper CE, Andrews SC. 2003. Global iron-dependent gene regulation in Escherichia coli. A new mechanism for iron homeostasis. J Biol Chem 278:29478-86.
72. Hantke K. 2003. Is the bacterial ferrous iron transporter FeoB a living fossil? Trends Microbiol 11:192-5.
73. Kammler M, Schön C, Hantke K. 1993. Characterization of the ferrous iron uptake system of Escherichia coli. J Bacteriol 175:6212-9.
74. Lau CK, Ishida H, Liu Z, Vogel HJ. 2013. Solution structure of Escherichia coli FeoA and its potential role in bacterial ferrous iron transport. J Bacteriol 195:46-55.
75. Massé E, Salvail H, Desnoyers G, Arguin M. 2007. Small RNAs controlling iron metabolism. Curr Opin Microbiol 10:140-5.
76. Balbontín R, Villagra N, Pardos de la Gándara M, Mora G, Figueroa-Bossi N, Bossi L. 2016. Expression of IroN, the salmochelin siderophore receptor, requires mRNA activation by RyhB small RNA homologues. Mol Microbiol 100:139-55.
77. Johnston NR, Strobel SA. 2020. Principles of fluoride toxicity and the cellular response: a review. Arch Toxicol 94:1051-1069.
78. Murashko ON, Yeh KH, Yu CA, Kaberdin VR, Lin-Chao S. 2023. Sodium Fluoride Exposure Leads to ATP Depletion and Altered RNA Decay in Escherichia coli under Anaerobic Conditions. Microbiol Spectr 11:e0415822.
79. Ratledge C. 2004. Iron, mycobacteria and tuberculosis. Tuberculosis (Edinb) 84:110-30.
80. Tsylents U, Burmistrz M, Wojciechowska M, Stępień J, Maj P, Trylska J. 2024. Iron uptake pathway of. Front Microbiol 15:1331021.
81. Postle K, Larsen RA. 2007. TonB-dependent energy transduction between outer and cytoplasmic membranes. Biometals 20:453-65.
82. Grosse C, Scherer J, Koch D, Otto M, Taudte N, Grass G. 2006. A new ferrous iron-uptake transporter, EfeU (YcdN), from Escherichia coli. Mol Microbiol 62:120-31.

83. Clarke TA, Dennison V, Seward HE, Burlat B, Cole JA, Hemmings AM, Richardson DJ. 2004. Purification and Spectropotentiometric Characterization of Escherichia coli NrfB, a Decaheme Homodimer That Transfers Electrons to the Decaheme Periplasmic Nitrite Reductase Complex*. Journal of Biological Chemistry 279:41333-41339.
84. Kranz RG, Richard-Fogal C, Taylor JS, Frawley ER. 2009. Cytochrome c biogenesis: mechanisms for covalent modifications and trafficking of heme and for heme-iron redox control. Microbiol Mol Biol Rev 73:510-28, Table of Contents.
85. Baez A, Sharma AK, Bryukhanov A, Anderson ED, Rudack L, Olivares-Hernández R, Quan D, Shiloach J. 2022. Iron availability enhances the cellular energetics of aerobic Escherichia coli cultures while upregulating anaerobic respiratory chains. New Biotechnology 71:11-20.
86. Erickson DW, Schink SJ, Patsalo V, Williamson JR, Gerland U, Hwa T. 2017. A global resource allocation strategy governs growth transition kinetics of Escherichia coli. Nature 551:119-123.
87. Jozefczuk S, Klie S, Catchpole G, Szymanski J, Cuadros-Inostroza A, Steinhauser D, Selbig J, Willmitzer L. 2010. Metabolomic and transcriptomic stress response of Escherichia coli. Mol Syst Biol 6:364.
88. Ren X, Wei Y, Zhao H, Shao J, Zeng F, Wang Z, Li L. 2023. A comprehensive review and comparison of L-tryptophan biosynthesis in Saccharomyces cerevisiae and Escherichia coli. Front Bioeng Biotechnol 11:1261832.
89. Santillan M, Zeron ES. 2004. Dynamic influence of feedback enzyme inhibition and transcription attenuation on the tryptophan operon response to nutritional shifts. J Theor Biol 231:287-98.
90. Hao R, Wang S, Jin X, Yang X, Qi Q, Liang Q. 2023. Dynamic and balanced regulation of the thrABC operon gene for efficient synthesis of L-threonine. Front Bioeng Biotechnol 11:1118948.
91. Wechsler JA, Adelberg EA. 1969. Antipolarity in the ilv operon of Escherichia coli K-12. J Bacteriol 98:1179-94.
92. Ponath F, Hor J, Vogel J. 2022. An overview of gene regulation in bacteria by small RNAs derived from mRNA 3' ends. FEMS Microbiol Rev 46.
93. Holmqvist E, Vogel J. 2018. RNA-binding proteins in bacteria. Nat Rev Microbiol 16:601-615.
94. Hor J, Matera G, Vogel J, Gottesman S, Storz G. 2020. Trans-Acting Small RNAs and Their Effects on Gene Expression in Escherichia coli and Salmonella enterica. EcoSal Plus 9.
95. Fitzgerald NJM, Simcik MF, Novak PJ. 2018. Perfluoroalkyl Substances Increase the Membrane Permeability and Quorum Sensing Response in *Aliivibrio fischeri*. Environmental Science & Technology Letters 5:26-31.
96. Fitzgerald NJM, Wargenau A, Sorenson C, Pedersen J, Tufenkji N, Novak PJ, Simcik MF. 2018. Partitioning and Accumulation of Perfluoroalkyl Substances in Model Lipid Bilayers and Bacteria. Environ Sci Technol 52:10433-10440.
97. McIlwain BC, Ruprecht MT, Stockbridge RB. 2021. Membrane Exporters of Fluoride Ion. Annu Rev Biochem 90:559-579.
98. Stockbridge RB, Robertson JL, Kolmakova-Partensky L, Miller C. 2013. A family of fluoride-specific ion channels with dual-topology architecture. Elife 2:e01084.

99. Qin J, Chai G, Brewer JM, Lovelace LL, Lebioda L. 2006. Fluoride inhibition of enolase: crystal structure and thermodynamics. Biochemistry 45:793-800.
100. McCormick NE, Jakeman DL. 2015. On the mechanism of phosphoenolpyruvate synthetase (PEPs) and its inhibition by sodium fluoride: potential magnesium and aluminum fluoride complexes of phosphoryl transfer. Biochem Cell Biol 93:236-40.
101. Zhou H, Zhang Y, Long CP, Xia X, Xue Y, Ma Y, Antoniewicz MR, Tao Y, Lin B. 2024. A citric acid cycle-deficient Escherichia coli as an efficient chassis for aerobic fermentations. Nat Commun 15:2372.
102. Yu BJ, Sung BH, Lee JY, Son SH, Kim MS, Kim SC. 2006. sucAB and sucCD are mutually essential genes in Escherichia coli. FEMS Microbiol Lett 254:245-50.
103. Förster AH, Gescher J. 2014. Metabolic Engineering of Escherichia coli for Production of Mixed-Acid Fermentation End Products. Front Bioeng Biotechnol 2:16.
104. Nikolaeva DD, Gelfand MS, Garushyants SK. 2021. Simplification of Ribosomes in Bacteria with Tiny Genomes. Mol Biol Evol 38:58-66.
105. Njenga R, Boele J, Öztürk Y, Koch H. 2023. Coping with stress: How bacteria fine-tune protein synthesis and protein transport. J Biol Chem 299.
106. Marquis RE. 1995. Antimicrobial actions of fluoride for oral bacteria. Can J Microbiol 41:955-64.
107. Goldberg AL, Moerschell RP, Chung CH, Maurizi MR. 1994. ATP-dependent protease La (lon) from Escherichia coli. Methods Enzymol 244:350-75.
108. Lee I, Suzuki CK. 2008. Functional mechanics of the ATP-dependent Lon protease-lessons from endogenous protein and synthetic peptide substrates. Biochim Biophys Acta 1784:727-35.
109. Luo S, McNeill M, Myers TG, Hohman RJ, Levine RL. 2008. Lon protease promotes survival of Escherichia coli during anaerobic glucose starvation. Arch Microbiol 189:181-5.
110. Kuroda A, Nomura K, Ohtomo R, Kato J, Ikeda T, Takiguchi N, Ohtake H, Kornberg A. 2001. Role of inorganic polyphosphate in promoting ribosomal protein degradation by the Lon protease in E. coli. Science 293:705-8.
111. Wilkens S. 2015. Structure and mechanism of ABC transporters. F1000Prime Rep 7:14.
112. de Keyzer J, van der Does C, Driessen AJ. 2003. The bacterial translocase: a dynamic protein channel complex. Cell Mol Life Sci 60:2034-52.
113. Sanganna Gari RR, Chattrakun K, Marsh BP, Mao C, Chada N, Randall LL, King GM. 2019. Direct visualization of the E. coli Sec translocase engaging precursor proteins in lipid bilayers. Sci Adv 5:eaav9404.
114. Chatzi KE, Sardis MF, Economou A, Karamanou S. 2014. SecA-mediated targeting and translocation of secretory proteins. Biochim Biophys Acta 1843:1466-74.
115. Natale P, Bruser T, Driessen AJ. 2008. Sec- and Tat-mediated protein secretion across the bacterial cytoplasmic membrane--distinct translocases and mechanisms. Biochim Biophys Acta 1778:1735-56.
116. Saibil H. 2013. Chaperone machines for protein folding, unfolding and disaggregation. Nat Rev Mol Cell Biol 14:630-42.
117. Bukau B, Walker GC. 1989. Cellular defects caused by deletion of the Escherichia coli dnaK gene indicate roles for heat shock protein in normal metabolism. J Bacteriol 171:2337-46.

118. Storey JM, Storey KB. 2023. Chaperone proteins: universal roles in surviving environmental stress. Cell Stress Chaperones 28:455-466.
119. Yadav A, Vuković L, Narayan M. 2024. An Atomic and Molecular Insight into How PFOA Reduces α-Helicity, Compromises Substrate Binding, and Creates Binding Pockets in a Model Globular Protein. Journal of the American Chemical Society 146:12766-12777.
120. Xu M, Cui Z, Zhao L, Hu S, Zong W, Liu R. 2018. Characterizing the binding interactions of PFOA and PFOS with catalase at the molecular level. Chemosphere 203:360-367.
121. Sutherland C, Murakami KS. 2018. An Introduction to the Structure and Function of the Catalytic Core Enzyme of. EcoSal Plus 8.
122. De Las Penas A, Connolly L, Gross CA. 1997. The sigmaE-mediated response to extracytoplasmic stress in Escherichia coli is transduced by RseA and RseB, two negative regulators of sigmaE. Mol Microbiol 24:373-85.
123. Paget MS. 2015. Bacterial Sigma Factors and Anti-Sigma Factors: Structure, Function and Distribution. Biomolecules 5:1245-65.
124. Darwin AJ. 2005. The phage-shock-protein response. Mol Microbiol 57:621-8.
125. Jones SE, Lloyd LJ, Tan KK, Buck M. 2003. Secretion defects that activate the phage shock response of Escherichia coli. J Bacteriol 185:6707-11.
126. Raetz CR, Guan Z, Ingram BO, Six DA, Song F, Wang X, Zhao J. 2009. Discovery of new biosynthetic pathways: the lipid A story. J Lipid Res 50 Suppl:S103-8.
127. Naumann A, Alesio J, Poonia M, Bothun GD. 2022. PFAS fluidize synthetic and bacterial lipid monolayers based on hydrophobicity and lipid charge. J Environ Chem Eng 10.
128. Colin R, Ni B, Laganenka L, Sourjik V. 2021. Multiple functions of flagellar motility and chemotaxis in bacterial physiology. FEMS Microbiol Rev 45.
129. Abdelwahed EK, Hussein NA, Moustafa A, Moneib NA, Aziz RK. 2022. Gene Networks and Pathways Involved in Escherichia coli Response to Multiple Stressors. Microorganisms 10.
130. Laganenka L, Colin R, Sourjik V. 2016. Chemotaxis towards autoinducer 2 mediates autoaggregation in Escherichia coli. Nat Commun 7:12984.
131. González Barrios AF, Zuo R, Hashimoto Y, Yang L, Bentley WE, Wood TK. 2006. Autoinducer 2 controls biofilm formation in Escherichia coli through a novel motility quorum-sensing regulator (MqsR, B3022). J Bacteriol 188:305-16.
132. Weathers TS, Higgins CP, Sharp JO. 2015. Enhanced biofilm production by a toluene-degrading Rhodococcus observed after exposure to perfluoroalkyl acids. Environ Sci Technol 49:5458-66.
133. Harbor CS. 2010. M9 minimal medium (standard). Cold Spring Harb Protoc 2010.
134. team P. 2022. RStudio: Integrated Development Environment for R., Posit Software, PBC, Boston, MA. http://www.posit.co/.
135. Team RC. 2022. R: A Language and Environment for Statistical Computing, R Foundation for Statistical Computing, Vienna, Austria. https://www.R-project.org/.
136. Institute TB. Trim Galore. https://github.com/FelixKrueger/TrimGalore. Accessed
137. Martin M. 2021. Cutadapt Removes Adapter Sequences From High-Throughput Sequencing Reads. EMBnetJournal 17.
138. Andrews S. 2010. FastQC: A Quality Control Tool for High Throughput Sequence Data [Online].

139. Thakur V. 2024. RNA-Seq Data Analysis for Differential Gene Expression Using HISAT2-StringTie-Ballgown Pipeline. Methods Mol Biol 2812:101-113.
140. Danecek P, Bonfield JK, Liddle J, Marshall J, Ohan V, Pollard MO, Whitwham A, Keane T, McCarthy SA, Davies RM, Li H. 2021. Twelve years of SAMtools and BCFtools. Gigascience 10.
141. Pertea M, Pertea GM, Antonescu CM, Chang TC, Mendell JT, Salzberg SL. 2015. StringTie enables improved reconstruction of a transcriptome from RNA-seq reads. Nat Biotechnol 33:290-5.
142. Soneson C, Love MI, Robinson MD. 2015. Differential analyses for RNA-seq: transcript-level estimates improve gene-level inferences. F1000Res 4:1521.
143. Kanehisa M, Goto S. 2000. KEGG: kyoto encyclopedia of genes and genomes. Nucleic Acids Res 28:27-30.
144. Wu T, Hu E, Xu S, Chen M, Guo P, Dai Z, Feng T, Zhou L, Tang W, Zhan L, Fu X, Liu S, Bo X, Yu G. 2021. clusterProfiler 4.0: A universal enrichment tool for interpreting omics data. Innovation (Camb) 2:100141.
145. Karp PD, Paley S, Caspi R, Kothari A, Krummenacker M, Midford PE, Moore LR, Subhraveti P, Gama-Castro S, Tierrafria VH, Lara P, Muñiz-Rascado L, Bonavides-Martinez C, Santos-Zavaleta A, Mackie A, Sun G, Ahn-Horst TA, Choi H, Covert MW, Collado-Vides J, Paulsen I. 2023. The EcoCyc Database (2023). EcoSal Plus 11:eesp00022023.
146. Edgar R, Domrachev M, Lash AE. 2002. Gene Expression Omnibus: NCBI gene expression and hybridization array data repository. Nucleic Acids Res 30:207-10.

Figures

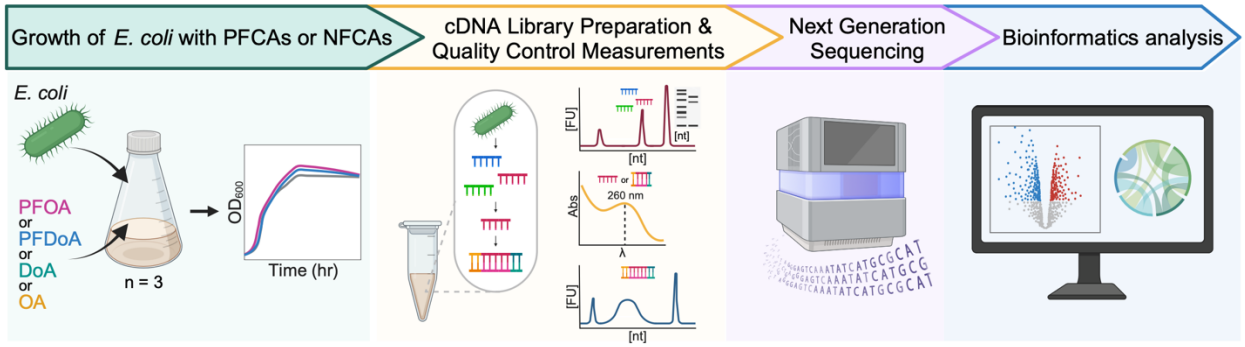

Figure 1. Experimental and computational workflow. This study characterizes the PFCA-induced transcriptional response of *E. coli* during mid-exponential phase and stationary phase growth. The schematic diagram of experimental design and data processing provides an overview of the growth of *E. coli* with PFCAs or NFCAs, microbial growth measurements, and cDNA library preparation and quality control measurements before next generation sequencing, bioinformatic data processing and differential expression analysis. Additional culturing and sampling information can be found in SI Figure 1.

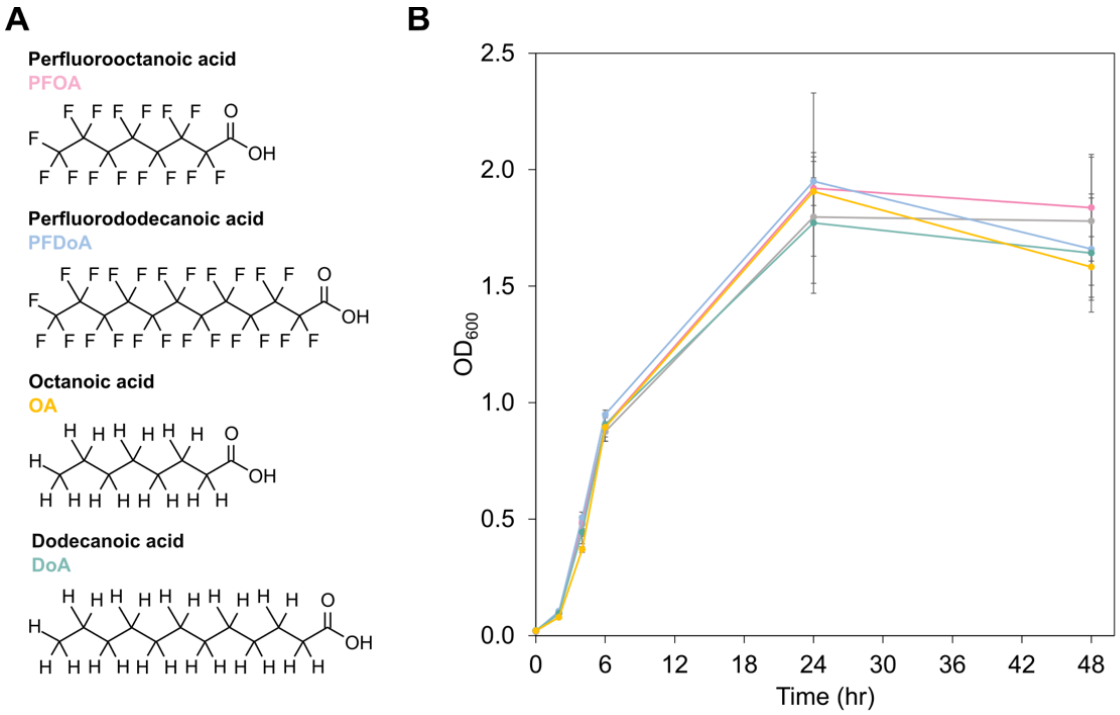

1068
1069
1070 **Figure 2. Growth of *E. coli* in the presence of PFCAs or NFCAs.** (A) Chemical structures of
1071 PFOA, PFDoA, OA, and DoA. (B) Growth of *E. coli* in M9 at 37 °C in the presence of 100 µmol/L
1072 of PFOA (pink), PFDoA, (blue), OA (yellow), or DoA (green) displayed as optical density
1073 measured at 600 nm (OD_{600}) over time (hr). Untreated cells containing an equivalent final
1074 concentration of DMSO are displayed in gray. Error bars represent one standard deviation of the
1075 mean value of biological triplicates (Table SI 1).
1076

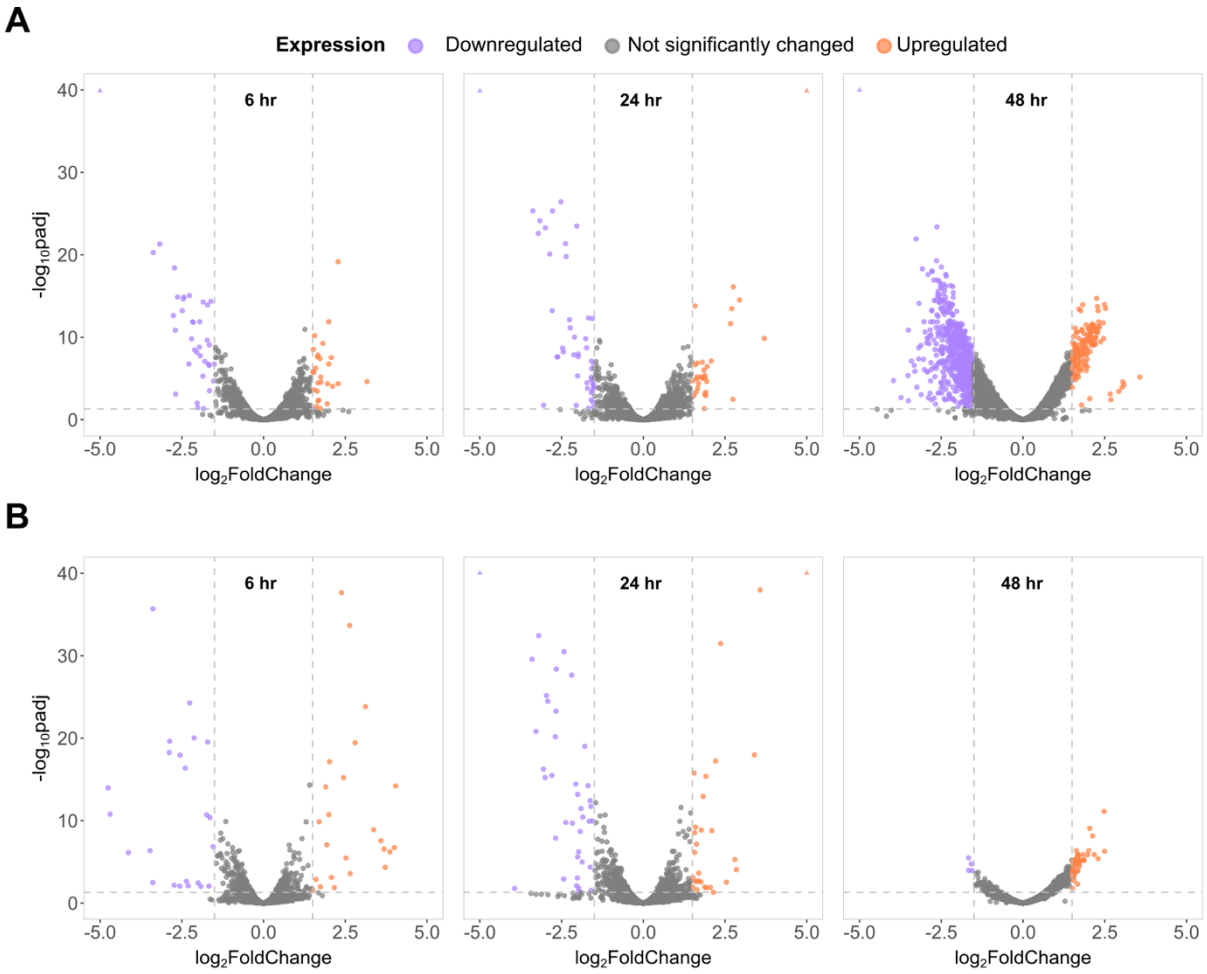

Figure 3. Transcriptomic profiles of mid-exponential and stationary phase *E. coli* grown with PFCAs. Volcano plots show the global transcriptional response of *E. coli* to (A) PFOA and (B) PFDoA in comparison to an untreated control group at 6 hr (left), 24 hr (middle), and 48 hr (right). Dashed lines represent a significance cutoff for differential expression of an adjusted p-value (padj) of less than 0.05 and absolute value of the $\log_2$ fold change greater than or equal to 1.5. Upregulated and downregulated genes are denoted by purple and orange, respectively, and genes not significantly changed by PFCA treatment are gray. Differentially expressed genes with $\log_2$ fold change and or padj values outside of the plot limits are represented by orange or purple triangles in the upper corners of each plot, if applicable.

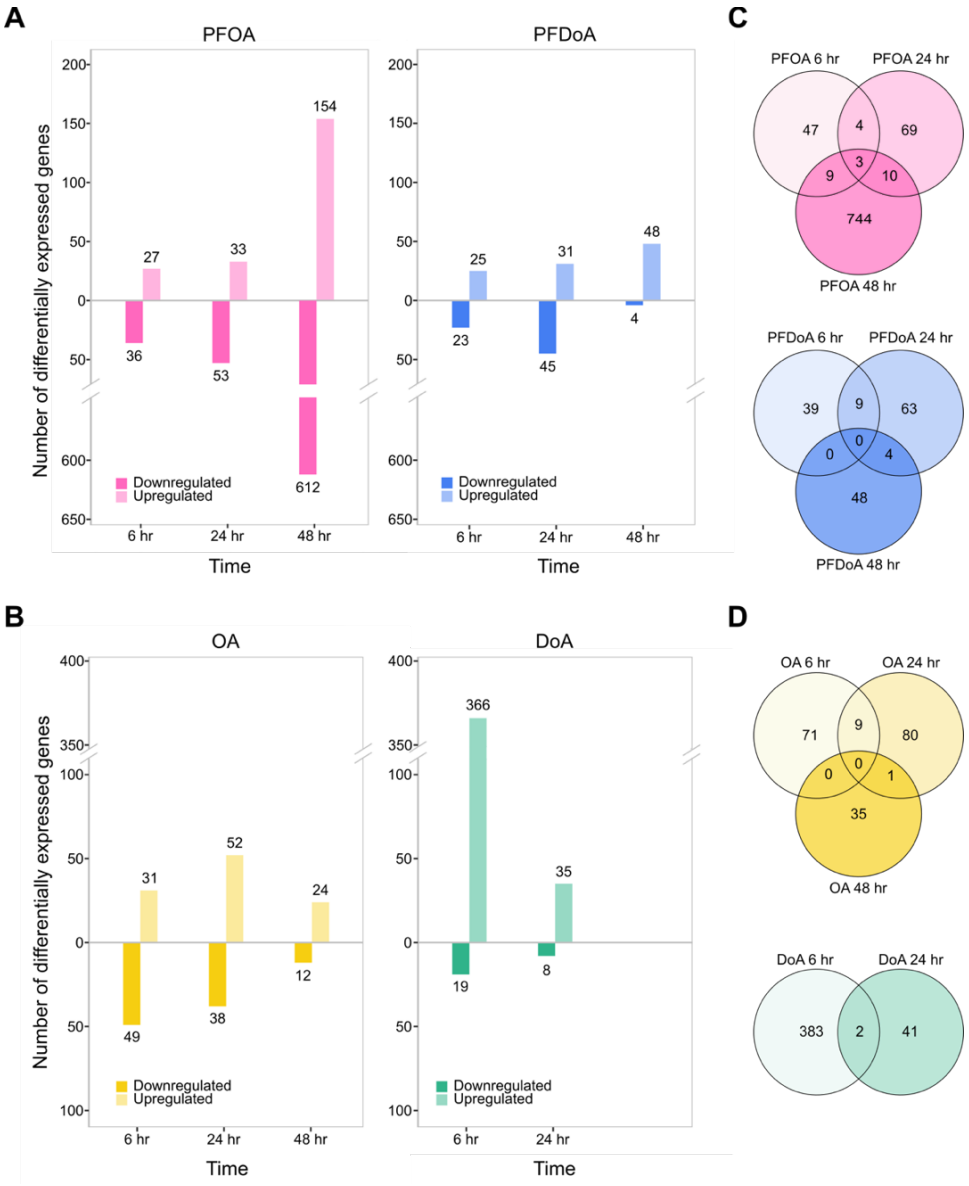

Figure 4. Comparison of differential gene expression of *E. coli* induced by PFCAs or NFCAs across the time course. The number of differentially expressed genes induced by (A) PFOA (pink, left), PFDoA (blue, right), (B) OA (yellow, left), and DoA (green, right) over the time course are shown by the height of each bar and label above or below the bar. Genes are considered differentially expressed if the absolute value of the $\log_2$ fold change greater than or equal to 1.5 and the adjusted p-value less than 0.05. Upregulated genes are represented by the upper portion of the plot with lighter shaded bars as indicated by the legend. Downregulated genes are represented by the lower portion of the plot with darker shaded bars. Venn diagrams display the number of differentially expressed genes induced by (C) PFOA (top), PFDoA (bottom), (D) OA (top), and DoA (bottom) over the time course. Unions display genes differentially expressed by one PFCA or NFCA at more than one time point. Genes in the outer circles are only differentially expressed at a single time point by one PFCA or NFCA.

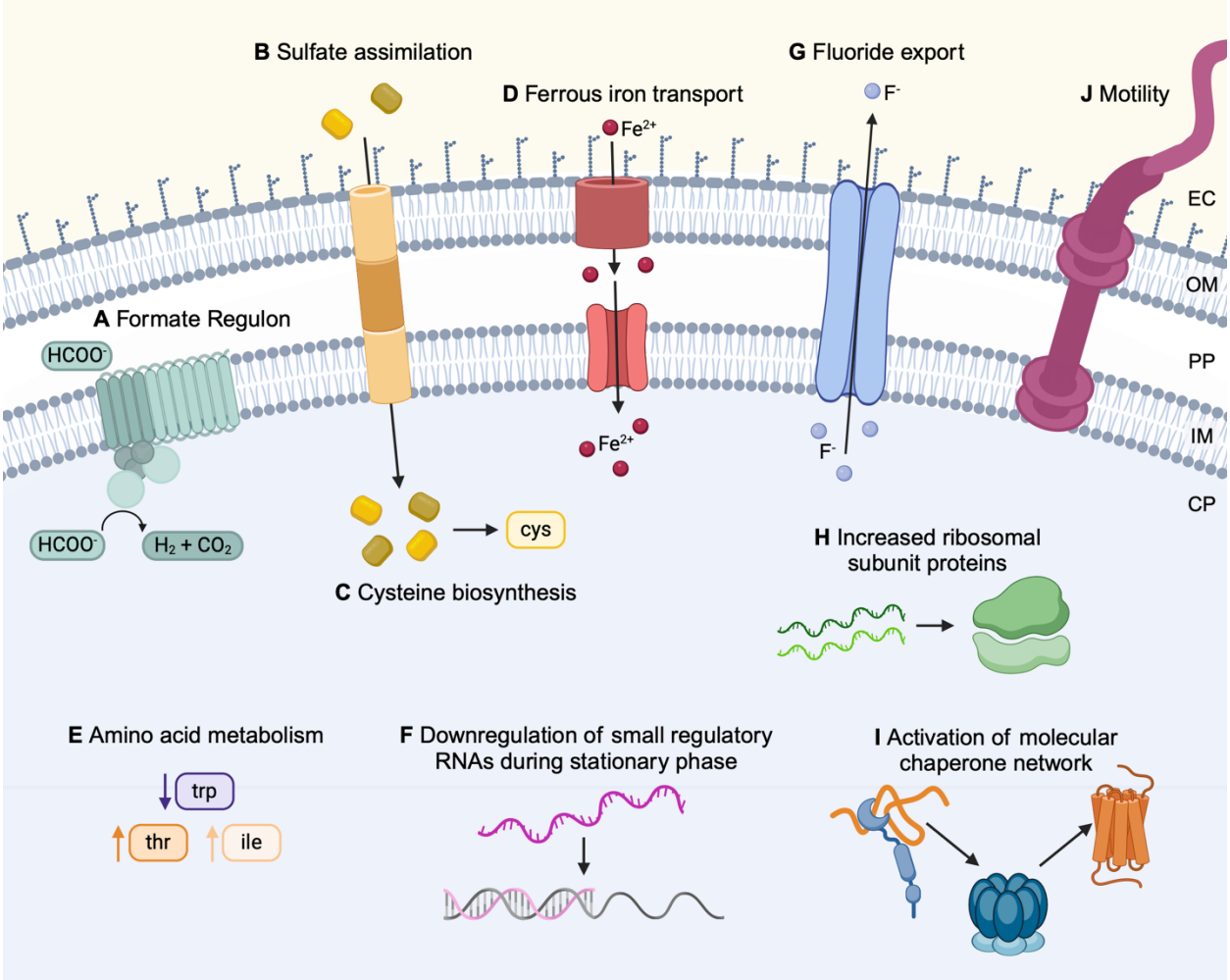

Figure 5. Schematic of key biological processes with altered gene expression in the presence of PFCAs across the time course. These processes are highlighted in the results and discussion. The formate regulon (A), sulfate assimilation (B), and cysteine biosynthesis (C) are discussed in the mid-exponential phase section. Ferrous iron transport (D), amino acid metabolism (E), and small regulatory RNAs (F) are discussed in the early stationary phase section. Fluoride export (G), ribosomal subunit proteins (H), the molecular chaperone network (I), and motility processes (J) are discussed in the late stationary phase section. The cytoplasm (CP), inner membrane (IM), periplasm (PP), outer membrane (OM), and extracellular environment (EC) are labeled on the right side of the schematic. The CP, PP, and EC have blue, white, and yellow backgrounds, respectively.

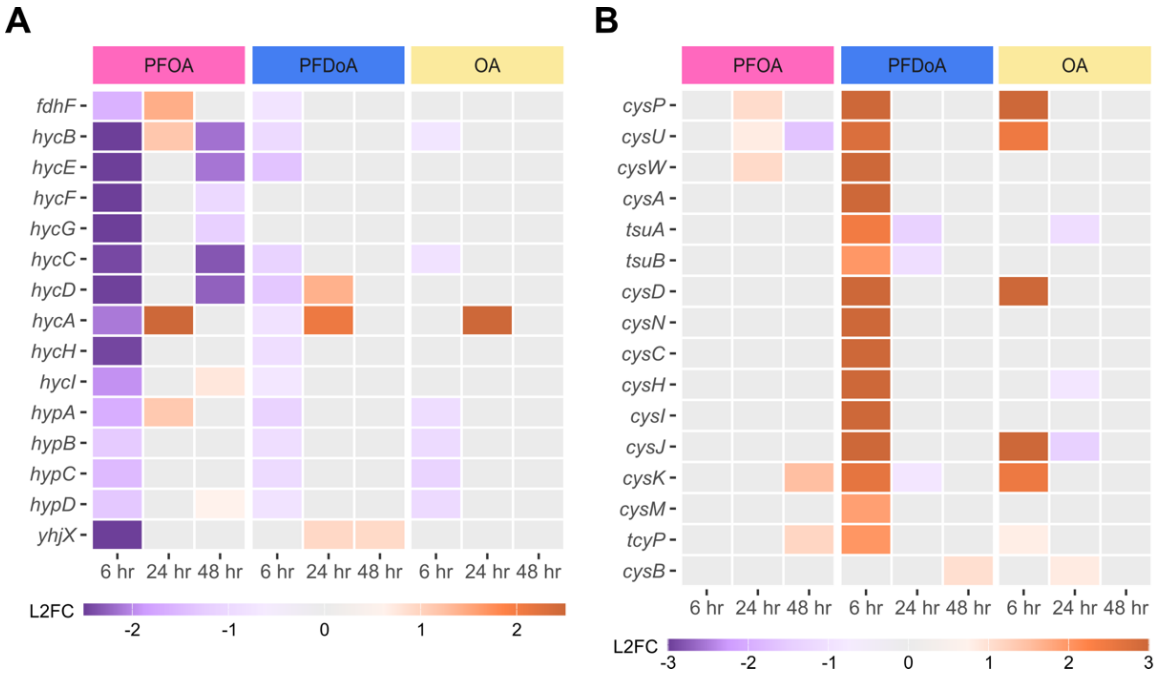

Figure 6. Select genes with differential expression at 6 hr and their temporal change. Heatmaps display differential expression of select genes (padj < 0.05) involved in (A) the formate regulon and (B) sulfate assimilation and cysteine biosynthesis. Expression is represented by $\log_2$ fold change (L2FC) within a gene compared to untreated control in a purple to orange scale displayed by legend color bar below each heatmap. Note heatmap color bars are different scales in (A) and (B) to best highlight differences. PFCA or NFCA treatment is represented by color coded bars at the top of the heatmaps: PFOA (pink), PFDoA (blue), and OA (yellow). Genes with no statistically significant change in expression are represented by gray boxes.

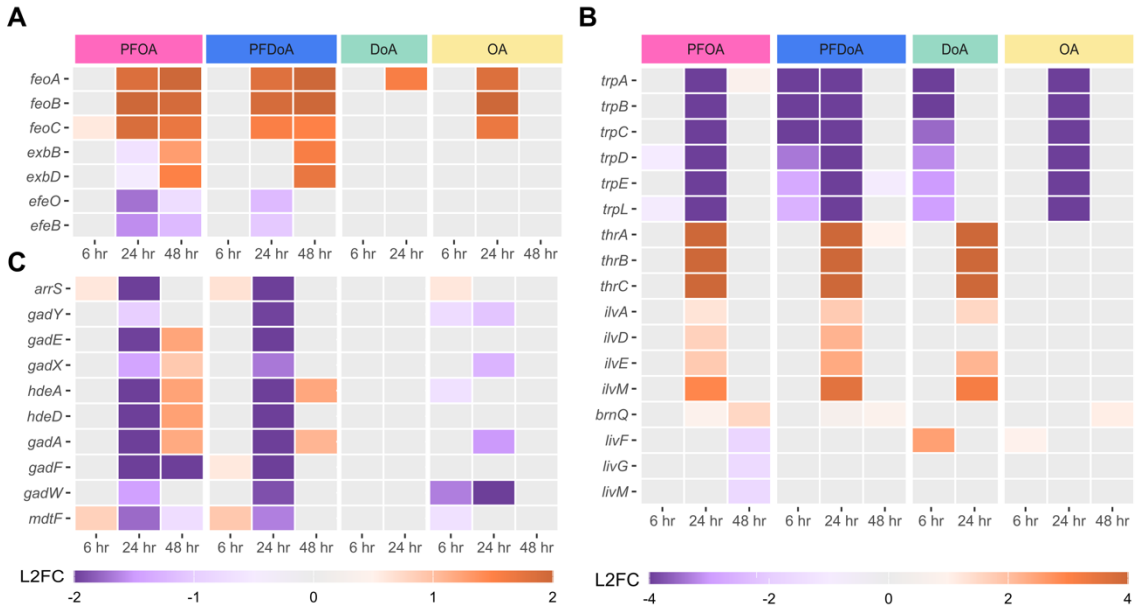

Figure 7. Select genes with differential expression at 24 hr. Heatmaps display differential expression of select genes (padj < 0.05) involved in (A) ferrous iron transport, (B) amino acid metabolism, and (C) small regulatory RNAs across the time course. Expression is represented by $\log_2$ fold change (L2FC) within a gene compared to untreated control in a purple to orange scale displayed by legend color bar below each heatmap. Note panels A and C share the same L2FC scale, which differs from panel B. PFCA or NFCA treatment is represented by color coded bars at the top of the heatmaps: PFOA (pink), PFDoA (blue), DoA (green), and OA (yellow). Genes with no significant change in expression are represented by gray boxes.

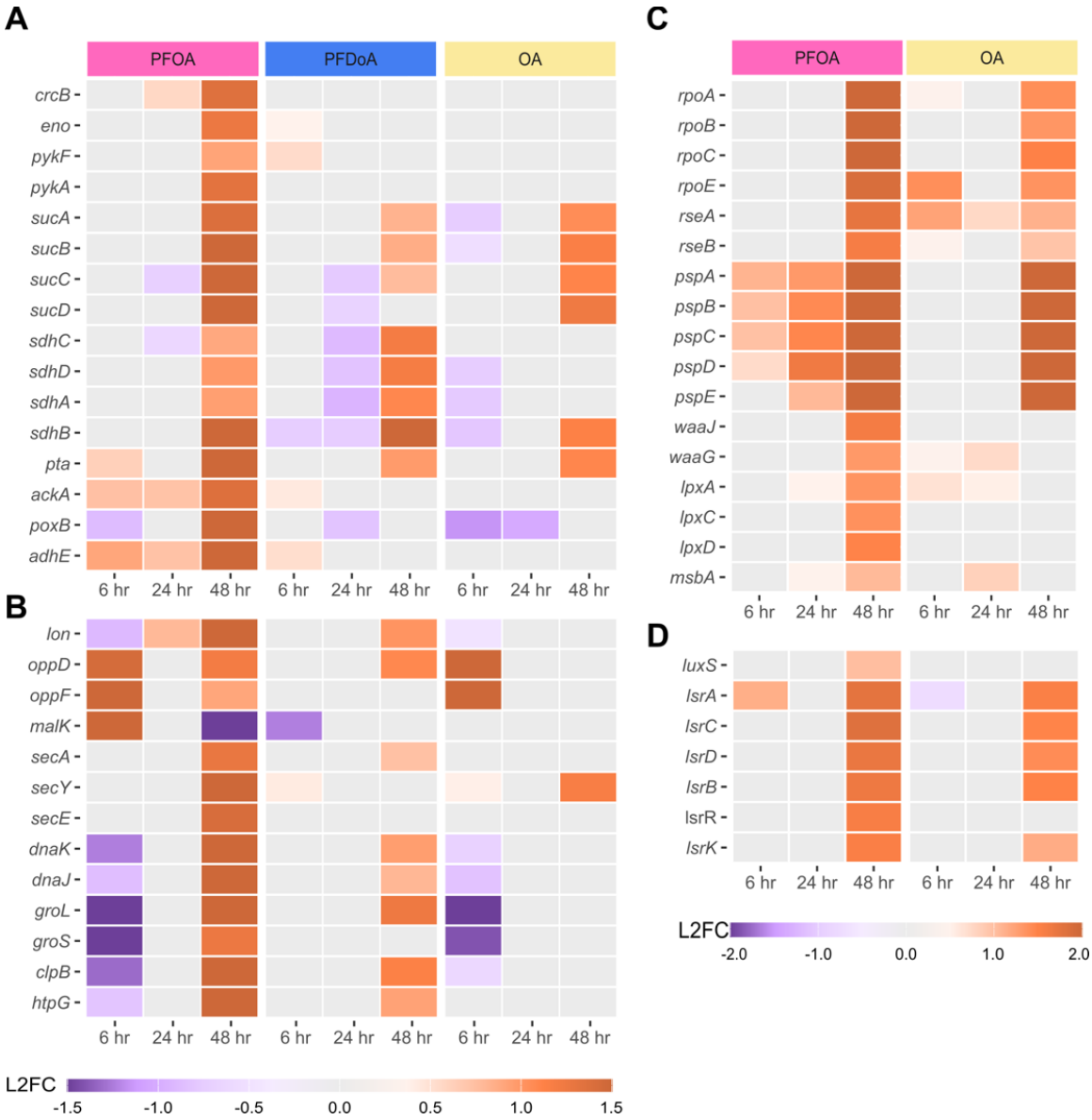

Figure 8. Select genes with differential expression at 48 hr. Heatmaps display differential expression of select genes (padj < 0.05) encoding (A) a fluoride exporter and metabolic enzymes, (B) ATPases and the molecular chaperone network, (C) sigma factors and envelope stress response, and (D) the AI-2 signaling system at select time points in the time course (6, 24, 48 hr). Expression is represented by $\log_2$ fold change (L2FC) within a gene compared to untreated control in a purple to orange scale displayed by legend color bar below each heatmap. Note heatmaps in A and B share the same L2FC scale and heatmaps in C and D share a separate scale. PFCA or NFCA treatment is represented by color coded bars at the top of the heatmap: PFOA (pink), PFDoA (blue), and OA (yellow). Genes with no significant change in expression are represented by gray boxes.